CHALMERS

Flow indication with a hydro turbine

- Process modeling and assessment of concept

Marcus Bilgec
Karl Lindell
Institution of signals and systems
Section for control technology, automation and mechatronics
CHALMERS INSTITUTE OF TECHNOLOGY
Gothenburg, Sweden, 2017

Bachelor's thesis 2017

Flow indication with a hydro turbine

A report containing studies and experiments on a small hydro turbine-generator to gain understanding of how the system can be upgraded and used as a flow meter.

Marcus Bilgec
Karl Lindell

Institution of signals and systems
CHALMERS INSTITUTE OF TECHNOLOGY
Gothenburg, Sweden 2017

Flow indication with a hydro turbine.
A report containing studies and experiments on a small hydro turbine-generator to gain understanding of how the system can be upgraded and used as a flow meter.
Marcus Bilgec
Karl Lindell

Supervisor and examiner: Göran Hult, Signals and systems

Bachelor's Thesis 2017
Department of Signals and Systems
Chalmers University of Technology
SE-412 96 Gothenburg
Telephone +46 31 772 1000

Cover: Turbine render image [15].
Printed by Serviceenheten Lindholmen
Gothenburg, Sweden 2017

Summary

Decentralized monitoring of the water supply network gives the opportunity to detect leakages in remote places early and thereby decrease operating cost and fresh water waste. This increases the need for flow meters and especially self-sustaining flow meters. The company where this bachelor thesis took place at is developing a small hydro turbine generator, applied in fresh water piping and used for supplying external measuring devices.

In this project, a method to convert the generator's output data to a corresponding flow have been developed. Surrounding factors' effect on the flow meter and its output have been evaluated.

Flow trials have been conducted to collect data on the turbine's rotational speed in relation to flow rate through the generator. The flow rate in relation to turbine blade angle and pipe size is mapped. Least squares approximation, interpolation and derivation of theoretical flow were considered for the conversion of registered generator output data to a corresponding flow. A feature for load shedding during low flow rate operation was implemented and evaluated through hardware trials.

Signal converting equations have been created using different methods. More flow trial data is needed for validation to conclude which method of signal conversion delivers the most accurate result. The theoretical approach was considered too inaccurate to be used alone and need to be supplemented with an approximated polynomial to reach acceptable results. The method for use of interpolation need validation using high quality flow trial data.

The possibility to use the generator as a flow meter is positive. Given optimal installation conditions of the flow meter, the output data varies with turbine geometry, pipe size, direction of change and electrical load, wherefore the modeling process must be repeated for different configurations. Instructions have been created to simplify this work for future turbine developments at the company.

Sammanfattning

Decentraliserad övervakning av vattenförsörjningsnätet ger möjlighet att upptäcka läckage tidigt i avlägsna områden och därigenom minska driftskostnaderna och spill av färskvatten. Detta ökar behovet av smarta flödesmätare, speciellt med en inbyggd funktion att strömförsörja sig själv. Det här examensarbetet har utförts hos ett företag som utvecklar en liten vattenturbin, som placeras i färskvattenledningar och används för att leverera energi till extern mätutrustning.

I detta arbete utvärderades möjligheten att använda generatorn som flödesmätare, såväl som omvigningsfaktorers inverkan på flödesmätaren och dess utsignal.

Datainsamlingar gjordes genom tester på olika flöden för att samla in data om turbinens rotationshastighet i förhållande till flödeshastigheten genom turbinen. Flödet är kartlagt i förhållande till turbinbladsvinkel och rörstorlek. Minsta kvadratmetoden, interpolering och en teoretisk härledning användes som olika metoder att ta fram modeller för flödet beroende på frekvensen. En funktion för lastsläppning vid låga flöden programmerades in och utvärderades genom hårdvarutester.

Signalkonverterande funktioner skapades med olika metoder. Mer flödesdata behövs för att validera och dra en slutsats vilken metod för signalomvandling ger minst fel. Den teoretiskt framtagna formeln ansågs ha för dålig precision för att användas ensam, varvid den kompletterades med ett approximerat polynom för att nå acceptabla resultat. Metoden som använder interpolering bör verifieras med flödesdata av hög kvalitet.

Möjligheten att använda generatorn som flödesmätare bedöms som god av författarna. Med optimala installationsförhållanden för flödesmätaren varierar utgångsdata med turbingeometri, rörstorlek, förändringsriktning av flödeshastighet och elektrisk belastning, varvid modelleringsprocessen måste upprepas för olika konfigurationer. Instruktioner har skapats för att förenkla detta arbete för framtida turbinutvecklingar hos företaget.

Acknowledgements

The authors of this bachelor thesis are very grateful for the hints, help and feedback that were provided throughout this project and necessary to complete the bachelor thesis.

First, we would like to thank Niklas Johansson and Martin Holm for the opportunity to become part of an interesting startup company for a few months, as well as providing feedback, company data and image material for the report. We would like to thank Martin for his inhouse supervision and guidance.

Big thanks to the company consultant Johan Linder for playing a crucial part of the development of the control system throughout these past months.

We would like to dedicate a thank you to the staff at the external test facility, for providing their hospitality and access to their test and measuring equipment in the early flow trials. Special thanks go to Styrbjörn Jonsson for operating the test equipment.

We are also thankful for the help from Reimond Emanuelsson and Anders Hildeman at Chalmers for providing input on trial methodology and Gunnar Byström at Swegon AB for input on how to attack the main scope of our thesis work.

We would like to give our thanks to Kjell Melkersson for providing an eye of correction with deriving mechanical problem.

We want to give our thanks to Alexander Ohm and Hafþór Pétursson who wrote their master thesis in applied mechanics at Chalmers parallel to us at the company, and provided some data from flow simulations. We also want to thank them for their input on the mechanics of fluid flow.

Finally, we would like to thank our supervisor and examiner Göran Hult for providing feedback on our work, guidance in how to address the problems and for providing measuring equipment from the institution.

Marcus Bilgec, Karl Lindell, Gothenburg, June 2017

Contents

List of Figures

Abbreviations

AGC	–	Automatic Generation Control
DAC	–	Digital-to-Analog Converter
DSP	–	Digital Signal Processing
GND	–	Ground
GTI	–	Grid Tie Inverter
IGBT	–	Insulated-gate bipolar transistor
LiPo	–	Lithium Polymer
LS	–	Least squares
MCT	–	Measurement and Control Technology
MCCP	–	Multiple-output Capture Compare PWM Module
MIPS	–	Million Instructions Per Second
Op Amp	–	Operation Amplifier
SRAM	–	Static random-access memory
TQFP	–	Thin Quad Flat Package
UART	–	Universal Asynchronous Receiver/Transmitter

1. Introduction

1.1. Background

Around 25% of the drinking water in an urban city's water supply is lost through leakage (see Figure 1). With a production cost at around 1 € per m^3 drinking water, the annual economic loss for the public sector is measured in billions. Only in Gothenburg, Sweden, the pipeline length is measured to 1750 km. And with a leakage rate of 23 %, an annual loss of 25,8 million € is caused by fresh water leakage in piping systems. This problem shows a potential to a decreased environmental impact and economic loss by detecting and serving leakages. By stationing flow meters throughout the water supply network and sending real-time data for decentralized monitoring, a flow drop between two adjacent flow meters can pinpoint a leakage in between. As a leak grow over time, a trend of increasing minimum flow reveals the error. This need for decentralized measuring is growing in the industry, with problems to solve for supplying remote sensors with energy and transmitting real time data [15].

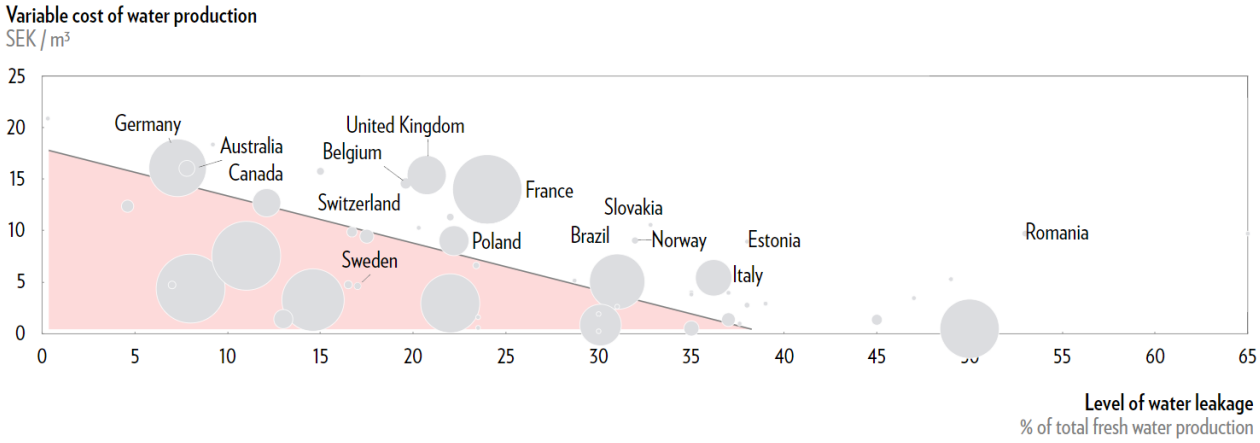

Figure 1: Bubble chart of water production cost and leakage in a few countries, where the bubble size represents the length of the pipeline network in each country. [15]

The company develops technology that enables remote measuring in the drinking water network. Using a synchronous generator with a hydro turbine, the company is developing a self-sustaining product that charges its own batteries and also supplies measurement devices, data loggers and flow meters with power. Now, the company wants to integrate the flow measurement as a feature in their product [15].

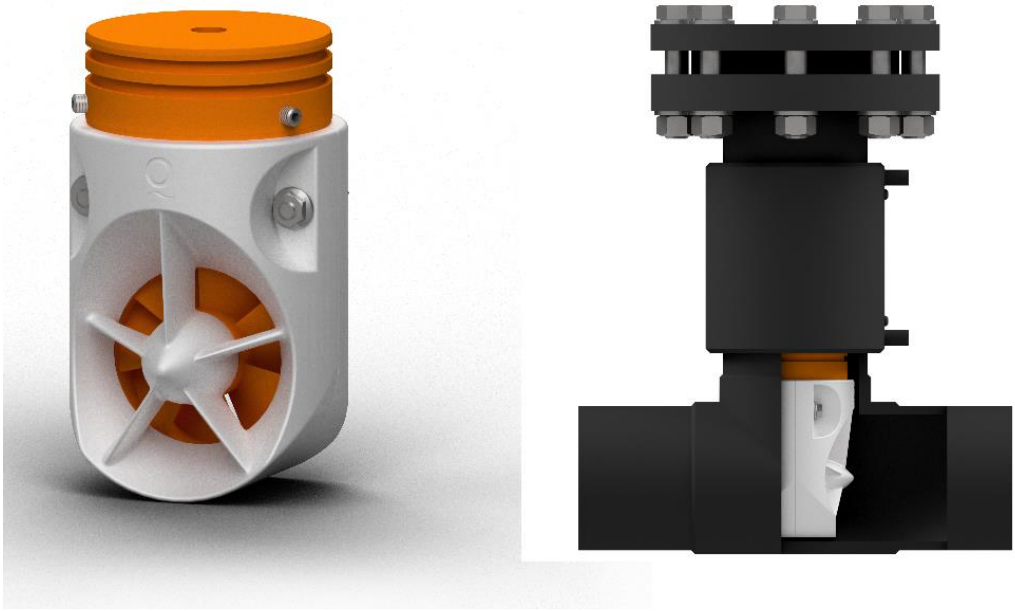

Figure 2: Rendering of the turbine and cross section rendering of turbine installed inside a T-pipe. [15]

1.2. Objectives

The main objectives of this project are:

1. To map turbine-generator signal output with respect to the water flow in the pipe.
2. Introduce a function to convert generator signal output to water flow with a maximum error of ±15%.
3. To implement the flow measurement function in an existing software.
4. Evaluate if the turbine can be used as a flow meter, taking in to account parameters with a significant impact on the output.

1.3. Purpose

The purpose with this project is to develop the software for a hydro turbine-generator control circuit with features to measure volume flow rate, hereafter referred to simply as *flow* in pipes during electricity generation.

1.4. Limitations

The project duration is between 2016-11-18 and 2017-06-31. Material and tools are provided by the department of Electrical Engineering at Chalmers and by the company. Equipment for testing is provided by external test facility and it is accessible for about four times during the project. The signal converter is created for a system of three standard pipe sizes positioned horizontally and with sufficient straight pipe length before and after the turbine. Water speed between 0.2 and 2.0 m/s are the most common flows and the converter should work in that

range. Most parts of the code will not be visible in this project to protect the content as well as the company name.

2. Theoretical references

This chapter contains information about existing products on the market for flow measurement, components used in this project, how a synchronous generator can be used to measure the flow, control of synchronous generator and processing output data.

2.1. Flow properties

Water flow can be measured properly if the fluid is homogenous and single-phased (i.e. same velocity of the fluid throughout a cross section and without air pockets/bubbles in the pipe) [9]. There are other properties of water as a flowing fluid in a piping system that need recognizing as surrounding factors of a turbine flow meter.

Water pressure in the pipes affect the turbines rotational speed through the force applied on the blades of the turbine [9]. The total pressure is the sum of the dynamic, static and hydrostatic pressure. The static pressure is pressure applied on the surfaces when the fluid is still, and lies at about 3-7 Bar in the product's intended environment [12][15]. Static pressure does not affect the generator output given for a given flow [15]. The dynamic pressure is the pressure caused by the motion of the fluid. The hydrostatic pressure is caused by an elevation difference of a fluid, and is not explained further since an elevation is not a problem in this case [12].

Dynamic viscosity is the flow resistance of the fluid [9][13]. The ratio of dynamic viscosity and water density is the kinematic viscosity [13].

Flow rate (Q) is the volumetric flow rate of the fluid, and is a product of the fluid's free-stream velocity (V_{inf}) and the flow area (A), i.e. cross-sectional area of unobstructed flow [9].

$$Q = V_{Inf}A$$

Equation 1: Flow rate.

The flow area changes over time due to corrosion and erosion in the pipe, and has according to Equation 1 a direct impact on flow speed given a constant flow [9].

Temperature of the fluid affect its viscosity, density and pressure [9]. The force applied axially on the turbine blade and result in the peripheral force F (see Appendix figure 5). The axial force on the blades are caused by the dynamic pressure force and the viscous force of the fluid. Since viscous force is determined by the kinematic viscosity of the fluid, which in turn is affected by temperature of the fluid, temperature variations may affect the rotational speed of the turbine and thus the measured flow [15]. According to [9], this creates a need for recalibration of flow meters during significant changes in temperature. This is further discussed in section 9.1.5.

2.1.1. Reynolds Number

A pump or gravity cause inertial forces when generating flow. The ratio of inertial forces to viscous forces (resistance to flow) give the Reynolds number (Re). Reynolds number is a dimensionless parameter that indicates which of the two forces dominates, and indicates whether the flow is laminar, transitional or turbulent. The number is determined by density (ρ), free-stream velocity (V_{inf}), pipe diameter (D) and fluid viscosity (μ) [9][22]:

2.1.2. Laminar and Turbulent flow

A fluid flowing through a pipe is seldom homogenous, but have different velocities depending on the distance from the pipe's inner wall [9]. This can be illustrated using a velocity profile, or gradient, as shown in Figure 3 below.

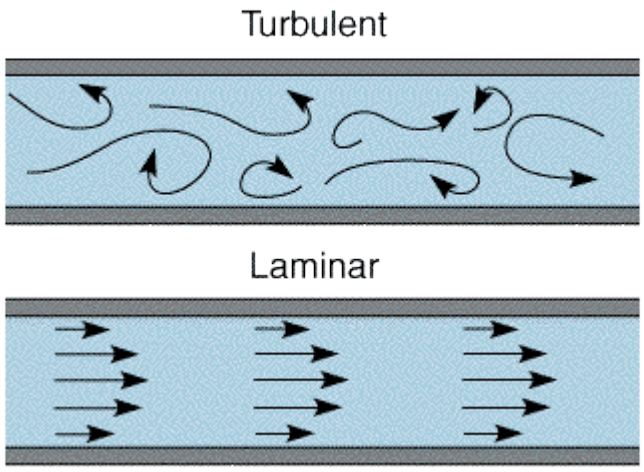

Figure 3: Turbulent and laminar flows. [17]

Flow can be laminar or turbulent depending on whether the flow is undisturbed or not [9]. Laminar flow is characterized by uniform velocity direction of fluid molecules have a *Re* value below 2300 [22] and transits gradually to turbulent flow when the velocity of the fluid reach the *transition flow*, with a *Re* value below 4000 [9][22]. Turbulent flow is characterized by randomly and irregularly fluctuating and gyrating fluid particles (as illustrated in the top of Figure 3) and a *Re* value above 4000, during which the fluid velocity fluctuates [9]. These fluctuations can, although small, have a great impact on flow characteristics [9]. Turbulence is common in the water industry, and steady flow can be represented using a mean velocity of the fluctuating velocity during turbulence [9]. Factors in circular pipes that increase the probability of transition from laminar to turbulent flow are pipe vibrations, flow velocity fluctuations in upstream flow and surface roughness.

2.1.3. Flow distortions and its causes

User manuals for pipe flow meters usually include instructions of minimal length of straight, or "undisturbed", pipe length before and after the flow meter. The lengths are usually multiples of the pipe diameter. The reason for these optimal installation conditions is to decrease distorted

velocity profiles, which complicates accurate flow measuring. It's therefore a significant problem when pipes have upstream/downstream flow, sharp curves or edges [9].

There are three typical types of distorted velocity profiles: skewed profile, swirl and flow separation. Skewed profile implicates an asymmetric velocity profile, with different velocity amplitudes of the otherwise parallel velocity vectors. Swirl emerge when the fluid molecules rotates around the pipe axis during flow. Flow separation emerge when the fluid passes over a sharp edge of a pipe fitting or enters a sharp corner of a pipe turn, where the flow separates from the pipe wall (see Figure 4 below) [9].

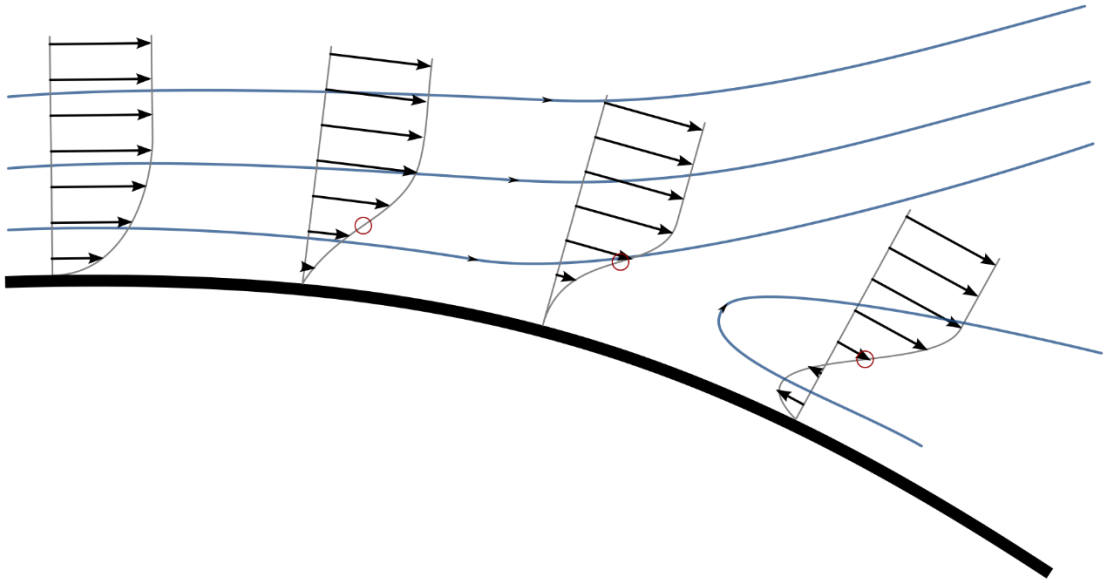

Figure 4: Flow separation in a pipe curvature. [14]

Propeller/turbine flow meters counter distorted velocity profiles partially by using stator blades as a partial function of the suspension of the rotor (See the right image of Figure 2). This straightening function is called flow conditioning [9].

2.2. Flow meter properties

Transducer is a commonly used term for a measuring device, and is more precisely a device that converts one form of energy to another, in this case water flow to an electric signal [9]. Using transducers to measure a physical process accurately sets requirements on transducer properties. Below are short explanations of different properties to avoid misconception.

Precision error is an uncorrectable deviation randomly caused by the flow meters technology and limitations. It is statistically representative through a bell-shaped normal distribution [11]. *Bias error* is the difference between actual value and the average measured value. Bias error is bidirectional, and can hence be eliminated through subtraction or addition to the measured value [11]. Causes of bias error are e.g. progressive mechanical wear in moveable parts [5], uncorrected zero shift or device temperature sensitivity [11].

Often confused with precision, *accuracy* indicates how close the measured values agree with the actual. Accuracy is hence referred to as error, and is the ratio of the dispersion (difference between the actual and measured value) and the range of work (the difference between the maximum and minimum measurable flow). Manufacturers datasheets wrongly represent accuracy only as precision error, although accuracy consists of both precision error and bias error [11]. More on this matter is discussed in 9.1.7. In this work, error is defined as the ratio of the dispersion and the measured value, since the range of the product is unknown and will not be tested.

Sensitivity indicates how the bias error varies when a change of flow rate occurs and is established through a sensitivity coefficient as part of a mathematical relationship between input and output variables [11].

Transducer *speed* indicate the reaction time for output change after an input change. Flow meters have relatively high speeds in relation to the measured process, and the reaction time is hence negligible [5].

The relationship between a measured quantity and the transducer's output value is seldom characterized by perfect *linearity*, but often by an S-shaped curve, exponentially increasing or decreasing curve [5]. Linearization can be achieved both analogously or digitally, using a control circuit near a transducer [11] [5]. A digital linearization unit usually consists of a microprocessor with a built-in translation table to translate the input to a corresponding output value [5].

Repeatability is the transducers ability to give similar output values for a constant input value, and is, like error, represented as a percentage of the total range of measuring [11]. Repeatability is affected by unspecific physical effects [5].

Rangeability is defined as the ratio between the maximum and minimum actual flow, where a wide range is a positive but not always necessary property. The *range* is a specified flow interval in which a specific maximum error is met [11].

Traceability implies the quality of the flow meter's calibration in terms of documented chain of calibration that ends with a calibration authority [11][5].

2.3. Common flow meters

There are several ways to measure flow in pipes. This section describes some of the most common methods for measurement of water flow.

2.3.1. Turbine/propeller flow meter

Turbine/propeller meters usually have an error around 0.5 – 2 % from the actual flow. Turbine/propeller consist of a rotor which spins when the water hits the blades. The output quantity is either registered mechanically or digitally [10]. Flow velocity is proportional with the rotational speed of the turbine [9].

Turbine/propeller meters can be very accurate if calibrated frequently enough, and the analogue type need no external source of power [10].

This type of transducer needs maintenance and lubrication to maintain the maximum error over time. Also, these flow meters error increase for low flows, and they are sensitive to swirl and other disturbances in the pipe [10].

2.3.2. Differential-pressure meter

This method is commonly used due its simplicity, low cost and easy installation. Error lies mostly between 0.5 – 2 %. Differential-pressure meters commonly work by a reduced area in the pipe that accelerate the water and lowers the pressure in the pipe. The pressure is measured between normal pipe area and in the reduced area or after, and the flow speed can be calculated by the pressure difference [10].

This is a low-cost method to measure flow but it creates a permanent pressure loss in the pipe. It contains no moving parts which makes this equipment less dependent of maintenance and gives it a long life [10].

2.3.3. Magnetic flow meter

This method is commonly used due its minimal impact on the flow and the possibility to measure flows of low velocities. The error is around 0.5% with this method and it can measure flow speed down to 0.03 m/s. On an insulated area of the pipe a magnetic field is generated and the passing water is inducing a small electric current. The current increases proportionally to the flow velocity and thus the volumetric flow rate. This current is measured and calculated to the flow [10].

The method is good for measuring flows of low velocities and can be used on short pipes due a low sensitivity to swirl or other disturbances in the pipe. To be able to measure the flow the fluids electrical conductivity must be greater than 5 pS/cm [10].

2.3.4. Other methods commonly used [10]

- Transit time ultrasonic flow meters
- Vortex flow meter
- Acoustic flow meters
- Thermal flow meters

2.3.5. Communication

In some applications, the flow meter need to be able to communicate with other systems. There is analog signal transmission, e.g. by sending a current ranging from 4 to 20 mA, but binary (pulse) voltage signals between 1 to 5 V direct current is another option [18]. Digital transmission can be used and manufacturers allow different protocols for communication like HART, PROFIBUS, Modbus RS-485 among others [19] [20] [21].

2.4. Output signals of a synchronous generator

When the turbine rotor spins, it induces a current in the coils in the generator which result in an alternating current. The symmetrical three-phase system takes the form of three sine shaped waves with a phase shift of 120º, see Figure 5 [23]. The frequency of the signal has the following relationship with the generator/turbine rotational speed

$$f = \frac{nN}{60}$$

Equation 2: Synchronous generator frequency.

Where *n* is the generator/turbine rotational speed and *N* is the number of pole pairs on the rotor. Furthermore, the angular frequency, ω of the turbine is as follows [24].

$$\omega = \frac{2\pi n}{60}$$

Equation 3: Angular frequency.

Using ω in $\mathrm{rad/s}$, the turbine shaft power can be calculated as follows:

$$\mathrm{P} = \omega * \tau$$

Equation 4: Shaft power.

Where τ is the shaft torque in Nm [24]. Another significant mechanical property is efficiency (dimensionless). The product consists of a chain of mechanical and electrical subsystems (turbine, generator, rectifier etc.) with a separate efficiency. The efficiency of several subsystems in a chain can be combined into one efficiency simply by multiplying the efficiencies of each subsystem [28].

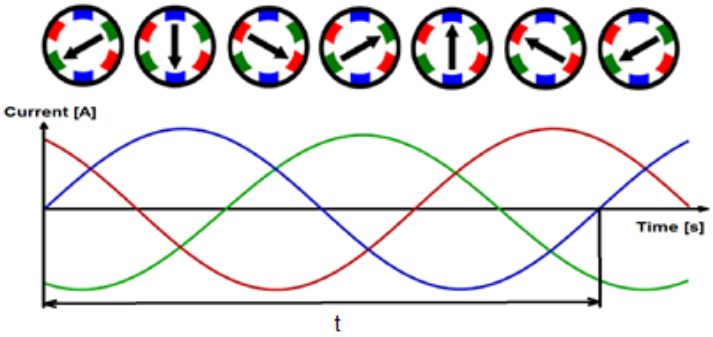

Figure 5: The basic principle of three-phase [25].

2.5. DIN Pipe standards

In Europe, the standard used for pipes is the DIN-system and the pipe diameter is referred to as DN or nominal diameter. In this report DN100, DN150 and DN200 are at focus because they are the most commonly used pipe sizes in the water supply network that needs monitoring [15].

2.6. Components

The product that the company is developing consists of a hydro turbine integrated in the rotor of a synchronous generator, which is connected to the generator control circuit. The product can supply power to several external instruments, e.g. an external data logger which is to receive and transmit data from the microcontroller.

2.6.1. Turbine and generator

The turbine wheel is integrated into the rotor of the generator, minimizing the number of moving parts to one. The current turbine consists of an axial reaction propeller, which is the most suitable type of hydro turbine in high pressure environments when kinetic as well as potential energy needs to be extracted [3].

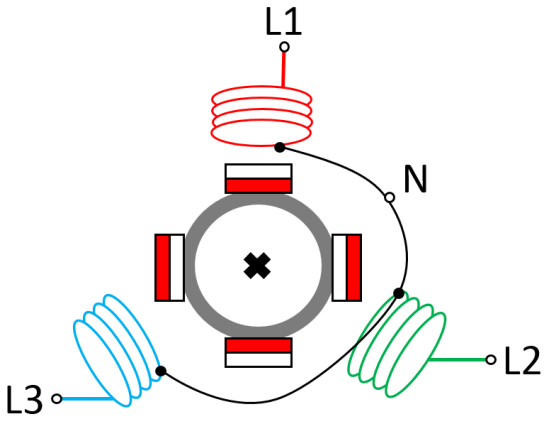

Figure 6: Three-phase synchronous generator diagram.

The generator consists of a rotor with permanent magnets mounted on the periphery of the turbine rotor, and a stator with coils coupled in three phase lines (marked with red, green and blue in Figure 6) with a wye-connection. The phase wires are connected to a full wave rectifier.

2.6.2. The control circuit

The hydro turbine generator is included with a circuit board. The control circuit handles rectifying phase voltages, receiving and analyzing of generator output data, battery charging, system status indication, communication with external devices that support modbus RTU.

The boards MCU is a 44 pin PIC24FV08KM204. It has the following significant features according to [6]:

- 2kB SRAM, 8kB flash program memory.
- 8 MHz internal oscillator.
- 16 MIPS CPU speed at 32 MHz clock input.
- 16-bit architecture.
- Requires a supply voltage of between 1.8 - 5.5 V. Can hence be directly supplied via LiPo battery cells.
- Two Op Amps, used for current measuring.
- Up to two 8-Bit DACs, used for DC-to-DC conversion.
- Ultra-Low-Power consumption.
- Three comparators, used for synchronous rectification.
- Tree MCCP modules, allows control of phase output signal through dead-time delay.
- UART module for interfacing.
- Low cost TQFP.

The control circuit is also equipped with a Sparkfun OpenLog datalogger that allows data storage. The storage system is an open source solution from Sparkfun that can save up to 64

GB of data to a micro SD memory card. The storage is integrated in a later prototype of the control circuit with a built-in logger with a micro SD card slot. The control circuit uses pulses to communicate with an external logger that is meant to send data to a central monitoring station. The pulse has a width of 30 ms and is sent when a set volumetric amount of water has passed. The amount of water that will pass are 25 liters per pulse as standard.

2.7. Control of synchronous generator

The Control circuit receives real time data of generated current, voltage and the three-phase frequency among other parameters. Generator frequency will hence be referred to as *fgen*, and is the main parameter used for output evaluation of the generator. When extracting power from a variable flow rate, control of the generator need to be addressed to create an optimal output [2]. In the case of this project, with a variable flow through the generator, load shedding or load adding is used for adjusting the electric current that is extracted from the generator to power selected loads. Load shedding keeps the turbine from stopping due to high electromagnetic torque. This breaking torque is caused by the electric load according to Faraday's Law, where the electrical loads, in this project includes battery cells in the control circuit and a constant resistive load. The external output is used for supplying other electrical circuits, allowing the control circuit to work as a transfer panel. Another important purpose of load shedding is to prevent overload the generator and thereby prevent short circuit [8].

Control of generator through load shedding/adding can be achieved with different types of control systems, e.g. digital signal processing (DSP), insulated-gate bipolar transistor (IGBT), grid tie inverter (GTI) or measurement and control technology (MCT) [2]. The Control circuit allows the generator to be controlled via DSP, which is more than capable of handling the task of real-time monitoring and regulation. Using a microcontroller (with its relatively small program memory) creates the potential for implementation of non-linear control systems, e.g. fuzzy-logic, using a control system that is advanced and yet require little memory [4].

fgen is measured in the Control circuit by using comparator to detect a phase pulse based on low or high phase voltage. Timer 1 is used in the microcontroller to measure the time between two leading edges of the phase pulses. Given a reasonable period, *fgen* is then calculated as the inverse of the period. *fgen* measured so that *fgen*/100 = measured frequency in Hz and the generated power, *Pgen*, is measured so that *Pgen*/1000 = generated power in W.

2.8. Data processing

There are numerous ways of processing values from an input data vector to a corresponding output data vector. The theory behind the methods is described here. All methods work as a "black box" (Figure 7) with the generator outputs, *fgen* and *Pgen* or only *fgen* as in signals and *flow* as output signals.

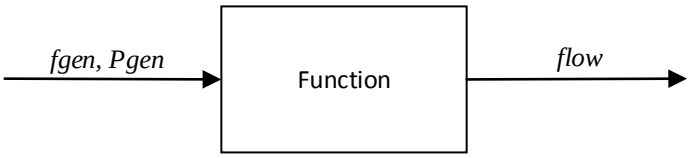

Figure 7 "black box"

2.8.1. Least-square Method

Least square method is used to approximate the polynomial via the function polyfit in MATLAB. It requires two vectors as input and what desired degree the polynomial should have. Polyfit(x,y,n) returns coefficients for a polynomial of n:th degree [26] on the form:

$$p(x) = p_1 x^n + p_2 x^{n-1} + \ldots + p_n x + p_n + 1.$$

Equation 5

This is later used to approximate functions.

2.8.2. Linear interpolation

Linear interpolation is shown in Figure 8, where f(C) and f(C-1) are two arbitrary points from a chart, using geometrical similarity of triangles, the ratio α is constant between the two points. Therefore, a value of Q_y can be calculated through interpolation, given a value of f_y. This is used to convert a measured frequency into a calculated flow.

$$\alpha = \frac{(f_y - f(C-1))}{(f(C) - f(C-1))}$$

Equation 6: Similarity of triangles.

$$Q_y = Q(C-1) + \alpha * (Q(C) - Q(C-1))$$

Equation 7: A value of flow through linear interpolation.

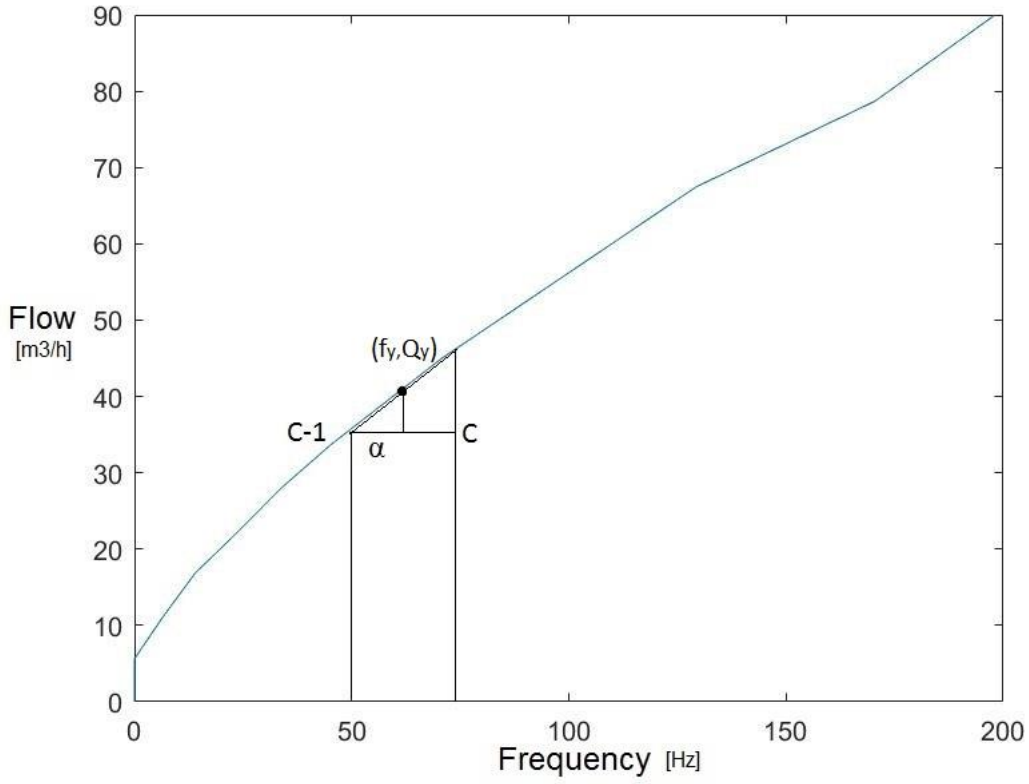

Figure 8: Principle of interpolation a value of flow.

3. Method

To accomplish the goals, this project was split in three main parts: data collection, data analyses and implementation.

3.1. Data collection

Data collections were made in flow and hardware trials where the turbine-generator system was tested and generator output data were registered. The flow trials were conducted in the product's intended environment. The process parameters of the flow trials were three different pipe sizes, electrical load on/off for flow velocities of 0.0 - 2.0 m/s of increasing/decreasing flow speed. Data collection was conducted in motor trials to verify data and to calculate the efficiency.

3.2. Methods of data processing

Four different methods were tested to create a feature to convert generator data to flow rate. Alternative A implies using a fully theoretical approach of converting generator power and frequency to a corresponding flow. Alternative B is the approximation of *flow* with a polynomial which is created using least squares (LS) from flow trial data with MATLAB. Alternative C is a combination of A and B where a theoretical flow is corrected with the difference between the theoretical value and the measured value. This bias error is represented with a polynomial. Alternative D is using interpolation on measured data to extract a flow rate value given a generator frequency.

All methods were tested in MATLAB and compared to the measured values to create an idea of how precise the turbine-generator system can be as a flow meter.

3.3. Implementation

To upgrade the generator into a flow meter, some features were added into the existing firmware of the product's control system. One function to turn off the electric load was created and another function to calculate the flow.

4. Data collection

The flow trials were conducted on three occasions to achieve a sufficient precision of the measuring feature. Two trials were conducted in external test facility.

4.1. Equipment for testing and recording

For this project, the frequency and the actual flow were the most significant parameters but generated power and pressure drop was also recorded. All equipment for testing and recording in this project is described below.

4.1.1. Meter laboratory, external test facility

The flow trials were carried out in a meter laboratory with a water pipe with similar properties to the product's intended environment. The equipment (see Figure 9) consists of a five meters long pipe directly coupled to the waterworks of Gothenburg, Sweden. The pipe had a manual steering valve for a variable flow, and was connected to a water tank for collection. Along the pipe length, an empty section of variable length was available for mounting the prototype, in our case a T-coupling in which the product is mounted through the vertical pipe. Volume flow rate was measured with a digital sensor connected to the water outlet. Pressure drop over the turbine was measured through two pressure gauges, of which one was analogue and placed before the turbine and the other one was digital (Proline Promag 53) placed after the turbine. With respect to customer requirements, the required range of flow speed for the test was covered by the facility, with an interval of 0,0 – 2,0 m/s. Flow velocity is used instead of volume flow in flow trial context to facilitate comparison between different pipe sizes, since the crossectional flow area affects the volume flow according to Equation 1.

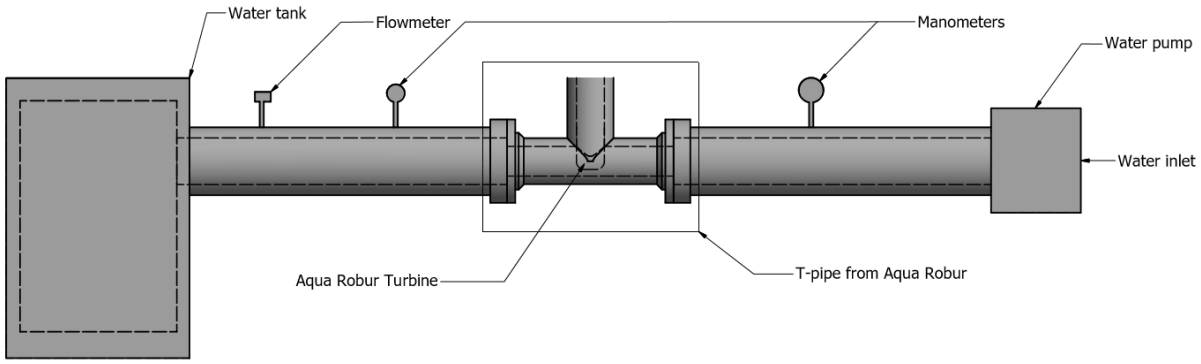

Figure 9: Test equipment at the external test facility

4.1.2. Motor rigs for hardware trials

Hardware tests were performed for data verification and minor component tests. In the beginning of this project, these tests were conducted by attaching the turbine rotor on the drill chuck of a BOSCH PBD 40 bench drill at the office. The stator was attachable to the vise, where

after a variable rotational speed, *n* could be set and verified with a AT-6 tachometer. The generator output could then measure frequency between two phase connectors on the synchronous generator's control circuit using a UNI-T UT61D multimeter.

The bench drill was later replaced with a SimplexMotion SM100A servomotor with SimplexMotionTool software for a more precise setting, monitoring and logging of shaft rotational speed, as well as shaft torque, motor current and voltage.

Throughout trials and hardware tests, the phase signal could be analyzed using a Rigol DS1052E oscilloscope. Minor electric measurement could be made on the system using the multimeter.

4.1.3. Proprietary flow trial rig

Due to the increasing need for testing new prototypes and achieving the goals of this project, a specific test rig was constructed which consisted of a looped piping system with a tank, a low pressure centrifugal pump and an inductive flow meter (see Figure 10). This would allow the company to collect more data with shorter notice and without administrative work of municipality cooperation.

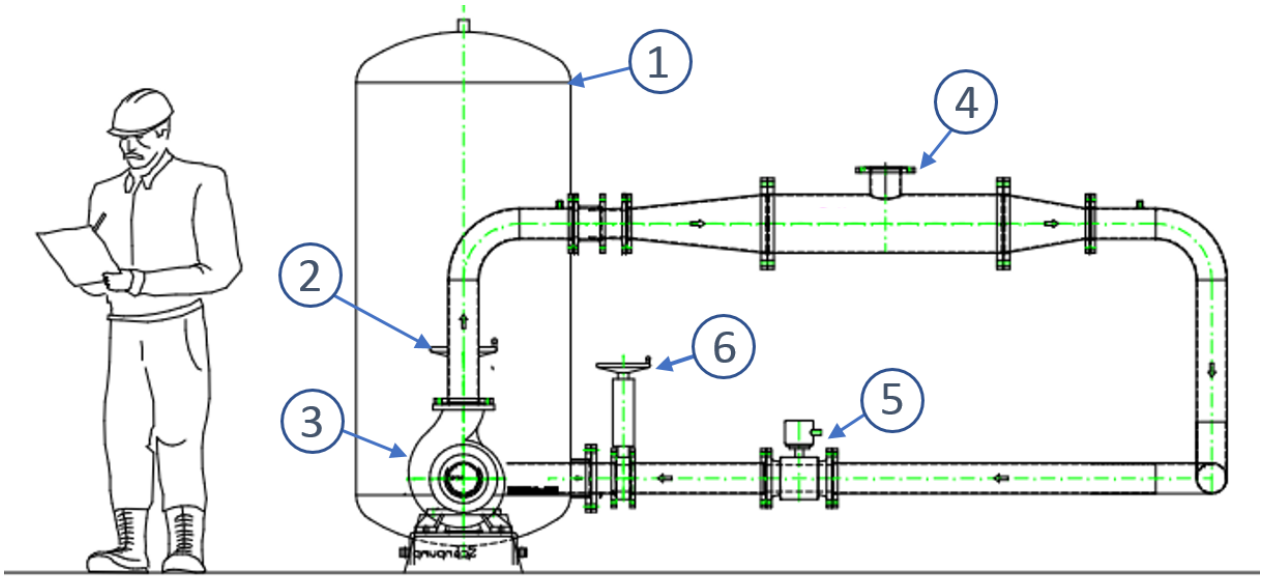

Figure 10: Proprietary flow trial rig [15].

The essential parts of the flow trial rigs are numbered as follows

1. Buffer tank, 500 liters.
2. Control valve, at tank outlet.
3. Centrifugal pump (ETB 125-100-160 GG AV11D300404 B).
4. T-pipe, for installing turbine.
5. Inductive flow meter (Waterflux 3000).

6. Butterfly valve, at tank inlet.

4.2. Conducted flow trials

The company have visited the external test facility before this project to conduct prototype tests, which allowed the authors to make preliminary assessments before the first data collection. Thereafter, two visits at the meter laboratory were carried out to gather suitable data to determine a relationship between generator rotational speed and pipe flow.

In flow trial 1, a five-bladed turbine wheel with a mean blade angle, hereafter referred to as "mid-angle" of 26.5°, was tested for DN150 and DN200 pipes. The generator phase lines were connected to a test rectifier with a 990 Ohm resistive load. For each measuring point, flow speed was increased with steps of 0,1 m/s, whereas steady state was achieved and an arbitrarily chosen mean voltage was measured after the rectifier and *fgen* were measured and noted in a prepared excel spreadsheet. The trial was aborted due to technical difficulties and data was collected from tests on DN150 and DN200. The results are summarized in section 7.1.1.

In flow trial 2, data was collected for three different pipe diameters using a new stator and mid-angle turbine. The pipe diameters were now DN100, DN150 and DN200, and the steps of flow speed increase were reduced to 0,05 m/s. Flow rate was measured on the test rig's flow meter by noting an arbitrarily chosen mean value. *fgen* was measured through the PC interface, where an arbitrarily chosen maximum and minimum value was noted. On occasion, the *fgen* register value on Simplex Interface was verified using the multimeter. All values were noted in a prepared spreadsheet. The results are summarized in section 7.1.2.

In flow trial 3, data was collected with the proprietary flow trial rig. The test did not result in measurements because of technical difficulties.

4.3. Conducted hardware trials

Two significant tests of the generator and the control circuit were made in the SimplexMotion motor rig.

The first trial was for verifying the implemented feature of load shedding, where generator shaft torque was measured through the motor shaft. The first part of load shedding verification was testing with and without an external load of 1 Ampere. The same procedure was repeated with deactivated and activated battery charging. Torque data were logged every 0.016 seconds in a total of four measure series, and a mean value of 500 elements were created to compare the breaking torque caused by the electrical load. Torque was measured with Simplex Motion tool. The results are compiled in Table 6.

The second trial was for measuring the efficiency of the path from turbine shaft to the PIC via the generator and rectifier, see Figure 11. The test was conducted by noting an intuitively chosen value of the shaft torque *T*, turbine rotational speed *n*, and generated power *Pgen* and for 7 different speeds.

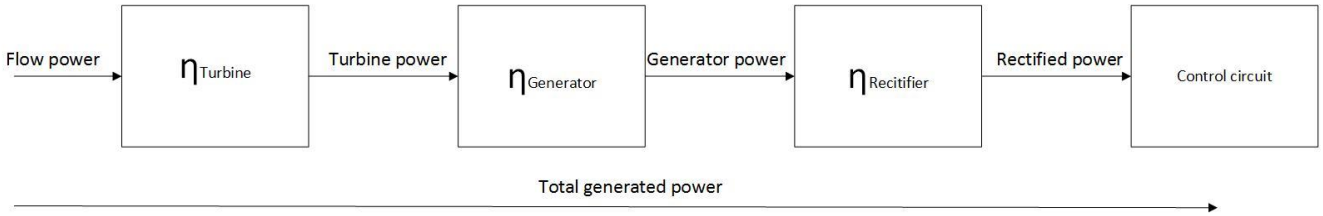

Figure 11: Powertrain from flow to electrical power in the control circuit.

The electrical efficiency was calculated by dividing registered *Pgen* with calculated turbine power. *Turbine power* was calculated using Equation 4, where *angular frequency* was calculated using Equation 3. The result can be viewed in section 7.2.2.

5. Methods of data processing

In this chapter, different methods are considered to create a "black box" using registered generator output data as input to determine *flow*. It also contains how the different methods used in the "black box" are evaluated.

The following approaches are concluded to be simple enough to analyze the flow trial data:

A. Using a theoretical approach, by implementing a derived function to convert a registered value of *fgen* and generator power, hence referred to as *Pgen,* to a corresponding value of *flow*.
B. Using the flow trial data to create and implement an approximative polynomial function with *flow* in respect to *fgen* in the control circuit, using least squares in MATLAB.
C. Using a combination of alternative A and B, i.e. to complete a theoretical function with a bias error function which is based on flow trial data.
D. Interpolation. Implementing a table of the flow trial data with *fgen* and *flow* into the control circuit, interpolation can be used to calculate an approximative value of *flow* between two measured points.

5.1. Alternative A - Theoretical approach

To reduce the need for testing and data collection, and hence cost and time consumption, a completely theoretical formula has been derived using a set of geometrical parameters to estimate a value of *flow* given a value of *fgen* and *Pgen.* This function will then be adapted to new turbine prototypes and different pipe installations. Using certain assumptions and simplifications, a function is derived (Appendix 2) and tested by comparing calculated *flow* to measured *flow* in MATLAB (see Figure 20).

Using the velocity triangle (see Appendix Figure 4) for turbomachinery, a simplified model describes the fluid flow as follows:

Equation 8 Theoretical function for flow from Appendix 2

$$Q_{Theory} = 900\pi\tan(\alpha)\left(D_{Blade,Outer}{}^2 + D_{Pipe}{}^2 - D_{Stator}{}^2 - D_{Blade,Inner}{}^2\right)\left(\frac{P_{Gen}}{F_{Blades,Outer}\eta_E} + \frac{D_{Blade,Outer}\pi f}{N}\right)$$

Where generator frequency and generated power are input variables. See Appendix 2 for parameter explanation and complete derivation of the function.

5.2. Alternative B - Approximative polynomial

The process of water flow through the turbine wheel was modeled using least squares approximation of vectors with stored trial data. After which, mathematical relationships were determined between different inputs on the system.

Using MATLAB, a script was made to collect measured data from excel and save it in the vectors "f" (*fgen)* and "Q" (*flow*). The script uses the function polyfit (see 2.8.1 for more information) to approximate a second-degree polynomial that fits the values. Polyval was used to create a new vector "Qc" for calculated *flow*. "Qc and "Q" is plotted in regard of "f". The MATLAB script can be found in Appendix 3 and the flowchart is found in Appendix 6. To verify the method, motor rig trials were used, see Appendix 10.

5.3. Alternative C - Combining theory and approximated polynomial

This method is based on the theoretical flow together with the measured values from the trials to create a two-part function. One part is the theoretical base where geometrical parameters from the existing generator can be inserted and the other part will be an approximative function of the bias error.

$$Q = Theoreticalflow(fgen, Pgen) + \ bias\ error(fgen)$$

Equation 9: Total flow rate, theoretical flow rate and bias error.

The script collects measured data from excel and saves it in the vectors "f" (*fgen),* "P_gen" (*Pgen)* and "Q" (*flow*). To make the data more intuitive, each element of "f" is divided by a factor of 100 to convert data vectors registered with the PIC into Hz. The geometrical input parameters (see section 5.1) are used, and a vector "Q_th" for the theoretical *flow,* is calculated from "f". Another vector "E_offset" have been created as the difference between "Q_th" and "Q". The MATLAB function polyfit (see 2.8.1 for more information) is used to approximate a second-degree polynomial that is used to fit the values of E_offset. The MATLAB function polyval is used to create a new vector "F" as an approximation of the error. The vector "Qtot" have then been created as a vector for the corrected flow values. The MATLAB script can be found in Appendix 4 and the flowchart is found in Appendix 6.

5.4. Alternative D - Using interpolation

This method has been tested using a MATLAB script and the measured values from the flow trials. A table is generated through plotted measure points from flow trial data, where a value of *flow* on the y-axis is given a through a value of *fgen* on the x-axis. Linear interpolation (explained in 2.8.2) is then used to retrieve intermediate values.

In the MATLAB script, two vectors "Q" and "f" are created containing elements equivalent to the values of *flow* and *fgen*. Another vector, "F" is created with values from 0 to 200 with equal steps to simulate 200 different frequencies to see how the plot looks like compared to reality. The script consists of two loops. The first loop processes each element of the vector "F" and the inner loop locates between which two nearby frequencies to interpolate. When the right values are found, the interpolation start and it saves a value to the vector "Flow" and

start again with the outer loop. For the full script, see Appendix 5 and for flowchart see Appendix 7.

Only the inner loop (see Appendix 7) is needed to calculate the *flow* and the outer loop is used to plot the measured values in MATLAB.

5.5. Evaluation of error

To validate how the methods perform, the maximum error and a mean error is calculated in relation to the measured values. This can be applied on Alternative A – C by comparing the calculated values to the measured values. The difference is calculated in percentage by calculating the difference between the calculated value and the measured value and divide by the measured value.

```
start = 1; %where to start calculating the error
E = start:length(f); %Error vector
Em = 0;

for x=start:length(f)
  E(x) = (abs(Q(x) - Qtot(x))/Q(x))*100 % Creates a vector with the error
 Em = E(x)/length(f) + Em %Calculates the mean error
end
```

6. Implementation

This chapter contains the programming and implementation of the function in the microcontroller. A function was added for measurement for the flow rate and releasing the electrical load on the generator. To enter the function, a mode named “mode 40” was created that allowed flow measurement to start.

6.1. Existing software

Since the start of this project there is an existing software with multiple functions. Among them is a function to communicate through a PC using a program called Simplex Interface. This is used for reading/writing to registers in the microcontroller. With simplex interface, the actual frequency, generator and battery voltage, generator and battery current and the generated power can be viewed among other parameters. During the project, a function to communicate the measured flow with an external logger have been created by a consultant.

6.1.1. Existing features

- Measure and filter the frequency, current, voltage.
- Calculate the generated power.
- Communicate via RS-485.
- Different operation modes, e.g. battery charging off, and Output voltage off.
- Two interrupts one on 1 kHz and one on 100 Hz.
- Check battery status and regulate the battery charging.
- Send pulses at the same frequency as *fgen*.

6.1.2. Interrupt

The code contains two interrupt routines running on 1 kHz and 100 Hz. The 1 kHz routine contained a loop that controlled the batteries and what mode is active. The slower 100 Hz routine handles the other functions to preserve energy. The 100 Hz can be seen in Figure 12**.**

```
306
307 // Interrupt handler to start code with lower priority 1.
308 // This code is less critical and will continue in the background. Not severe if overrun.
309 // Interrupt is triggered from the INT1 interrupt at a higher priority.
310 // This code is run at 100Hz rate
311 // Measured to take 195us (2%)
312 void __attribute__((interrupt, auto_psv)) _INT2Interrupt(void)
313 {
314     //PinIO2 = 0;
315     IFS1bits.INT2IF = 0;                    // Clear interrupt flag
316     AnalogUpdate();
317     StatusUpdate();
318     IndicatorUpdate();                      // Update indicator light blink pattern
319     FrequencyUpdate();                      // Calculate frequency
320     FlowrateUpdate();                       // Calculate the flow
321     BatteryUpdateSlow();
322     OutputUpdate();
323     LogUpdate();
324     //PinIO2 = 1;
325 }
```

Figure 12: 100 Hz Interrupt in Main.c.

6.1.3. Flow rate measurement

The existing code was modified with a complimentary function to calculate the *flow*. A set of new variables were created in the new parameter class "*Flow*". "*Flow"* is given the index value *140* in the register, and is used for writing and reading flow values via simplex interface. The functions contain the variables *FlowArea*, *FlowAngle*, *FlowRate*, *GenPower* and *GenFreq*. *GenFreq* and *GenPower* are returned in an already existing function and used in the the added flow indication feature. The new variables are declared in the file Parameters.h (Figure 13).

```
108 #define REG_FLOWRATE            140
109 //#define REG_FLOWAREA            141
110 //#define REG_FLOWANGLE           142
```

Figure 13 Declaration of variables in parameters.h

6.1.4. Communication

The microcontroller communicates with a PC through Simplex interface, a software created by an external consultant. RS-485 is used as communication standard. To enable reading from and writing to a parameter via simplex interface, corresponding registers in the program had to be altered. This had been achieved by adding variable name and register number into the register file (SimplexRegisters_Default) and adding the variable to an existing switch function in parameters.c (See Figure 14).

```
172         case REG_FLOWRATE: Param.FlowRate = Value; break; // Added by Marcus o Karl 170220
173         case REG_FLOWAREA: Param.FlowArea = Value; break; // Added by Marcus o Karl 170223
174         case REG_FLOWANGLE: Param.FlowAngle = Value; break; // Added by Marcus o Karl 170223
```

Figure 14: Code added to parameters.c.

6.2. Releasing the load and measuring the flow

A new mode, *MODE_FLOW seen in* Figure 15, have been created. When this mode is active, the flag *Flag.Flowrate* is set to one and the program will start to measure the flow. A function for flow measurement was implemented in the 100 Hz interrupt routine. Flowcharts can be seen in Appendix 8.

```
199             case MODE_FLOW:
200                 Flag.Active = True;
201                 Flag.Flowrate = True;
202                 break;
```

Figure 15: MODE_FLOW in main.c.

The function *FlowrateUpdate* is a "state machine" consisting of the following steps:

1. FlowStateStartup.
2. FlowStateStable.
3. FlowStateMean.
4. FlowStateCalculate.

This means that whenever *FlowrateUpdate* is called, it will continue from the last set state.

6.2.1. FlowStateStartup

At the start off the function *FlowrateUpdate* the program checks if *Flag.Flowrate* is set. If set, it will start a countdown timer at 50 seconds. When the timer hits zero, the program enters *MODE_FLOW* and turns off the battery charging using the function *Battery_off* which releases the load on the turbine. Then another timer is set to 5 seconds to let the flow get steady without any the impact of electrical load.

6.2.2. FlowStateStable

After 5 seconds, *fgen* is measured and compared to the previous *fgen*. If the difference is less than 0.2 Hz, the function continues. In other case, it leaves the function again to measure a new frequency, compare it with the previous value of *fgen* and repeat this until the difference is less than 0.2 Hz.

6.2.3. FlowStateMean

To measure a good value of the frequency, *fgen* is created from a mean value of frequencies measured in ten program cycles.

6.2.4. FlowStateCalculate

The *flow* is now calculated from that frequency. When a value of *flow* is returned, the countdown timer is set to 50 seconds again and the battery charger is reactivated, after which *FlowStateStartup* is set to next state.

6.3. Load shedding

To archive load shedding the function Battery_off and Battery_on is called upon. This function was a part of the existing code. When battery charge is off (*Battery_off*) K1 is open and K2 powers the external electronics, See Figure 16.

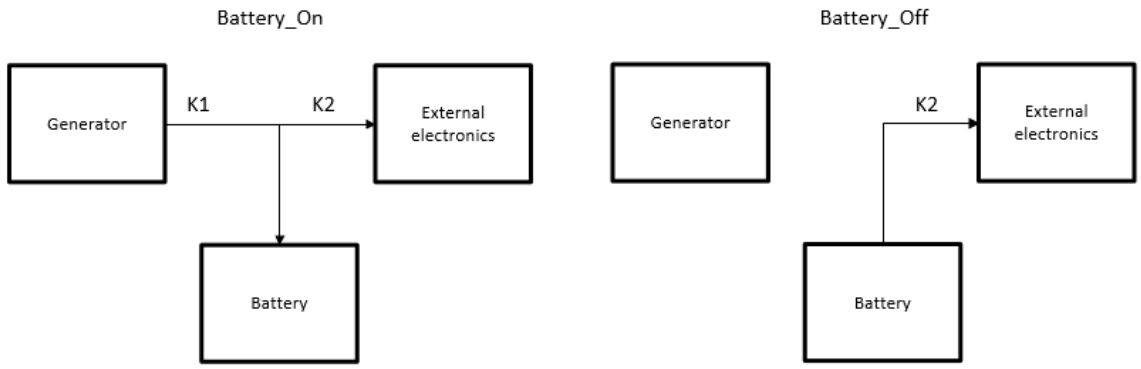

Figure 16: Battery charge on and off.

6.4. Implementation of alternatives:

To calculate the flow in FlowrateUpdate for alternative A – C a function can be added directly in to FlowrateUpdate. However, implementing alternative D with interpolation could look in the program code like the script in Figure 17.

```
f % datavector with measured values of frequency
Q % datavector with measured values of flow

while x <= length(f) %Second loop locates between what values to interpolate between
    if (FrequencyActual < f(x)) % when FrequencyActual > f(x) it should interpolate.
        c = x;
        x = lenght(f);
    end
 x = x + 1;
end
alpha = (F(y)-f(c-1))/(f(c)-f(c-1)); %Calculate the horizontal position
Flow(y) = Q(c-1)+alpha * (Q(c)-Q(c-1)); %Calculate the vertical position
```

Figure 17: Interpolation in microcontroller.

7. Result

This chapter contains some measured result from trial 1, trial 2 and hardware trials, together with the result from analyses of the data collections. The measured data consist of measured frequency and the flow rate measured by an external flow meter.

7.1. Conducted flow trials

Two out of three conducted flow trials provided sufficient data, and the significant observations are described in the following sections.

7.1.1. Flow trial 1

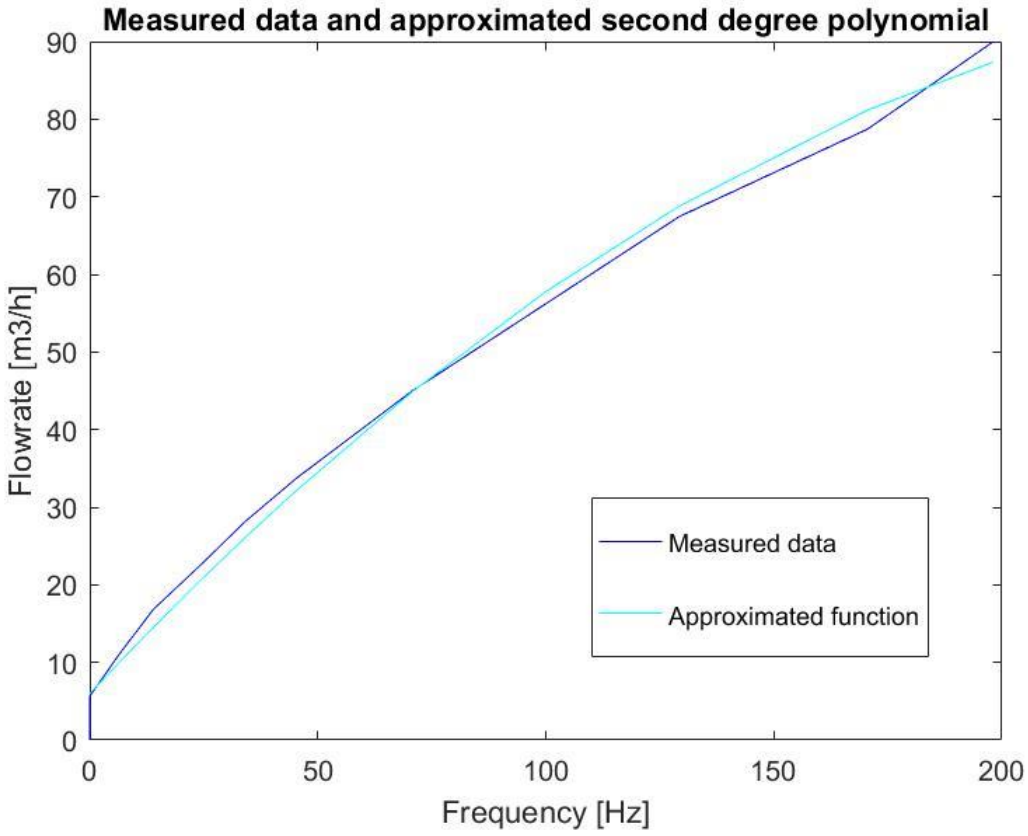

Figure 18: Alternative B for DN150 from trial 1.

The error was 13,7% at *fgen* = 14 Hz, which indicated a need for closer measure points at the between 0,0 and 45 m^3/h for DN150.

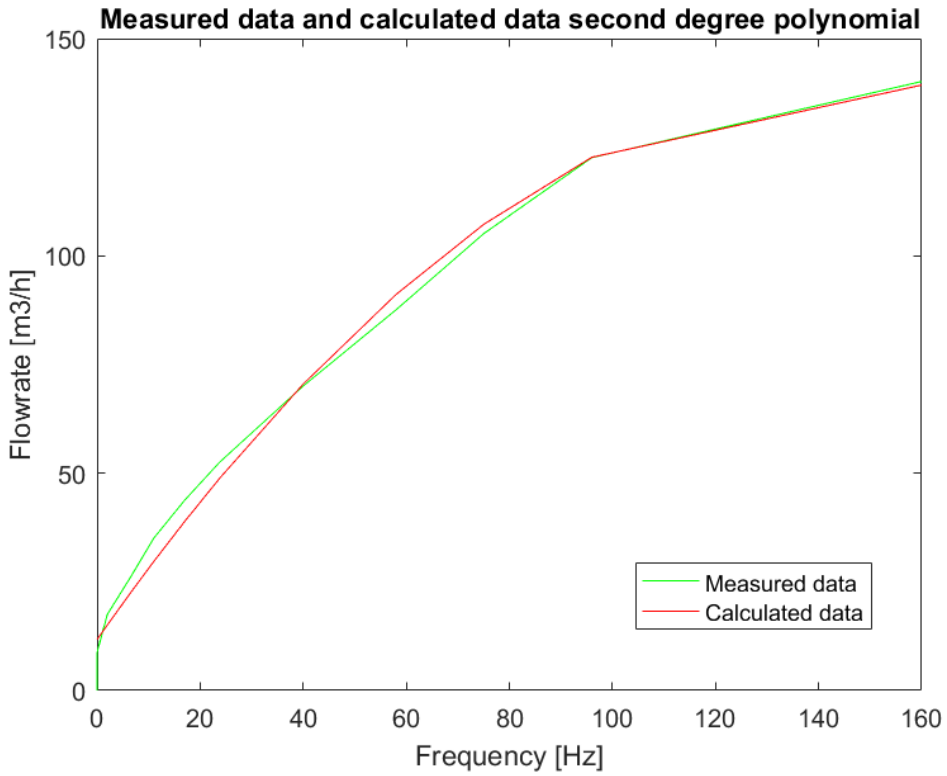

Figure 19: Alternative B for DN200 from trial 1.

The maximum error of corresponding approximation for DN200 is 15,3% at 11 Hz at 30 m^3/h. If a fourth-degree polynomial was used instead of a second-degree polynomial, the maximum error decreased to approximately 8% for both DN150 and DN200.

7.1.2. Flow trial 2

The result of flow trial 2 were data vectors of *flow* and *fgen* and *Pgen* for mid-angle turbine in DN100, DN150 and DN200. Using an oscilloscope, the phase signal over phase 1 and GND was verified free from interference during *MODE_FLOW* and *MODE_NORMAL*.

Table 1 shows variation of a mean maximum and mean minimum value of flow with and without battery charge and generated power. The number in brackets after the variation shows the number of measured values that the mean variation was calculated from.

Table 1: Result from trial 2.

	DN100	DN150	DN200
Absolute maximum/minimum Frequency with battery charge on [Hz]	117/15	141/10	75/7
Mean variation of frequency [Hz] with battery charge on (number of values)	0.96 (10)	1.92 (7)	1.45 (9)
Absolute maximum/minimum Frequency with no load [Hz]	117/16	141/11	101/73
Mean variation of frequency [Hz] without load (number of values)	0.82 (10)	0.87 (6)	1.62 (8)
Absolute maximum/minimum generator power [mW]	31/800	28/not valid	20/970
Mean variation of generated power [mW]	59 (10)	40 (9)	32 (6)

Figure 20 below shows a graph of the measured and theoretical flow respectively for DN100, DN150 and DN200.

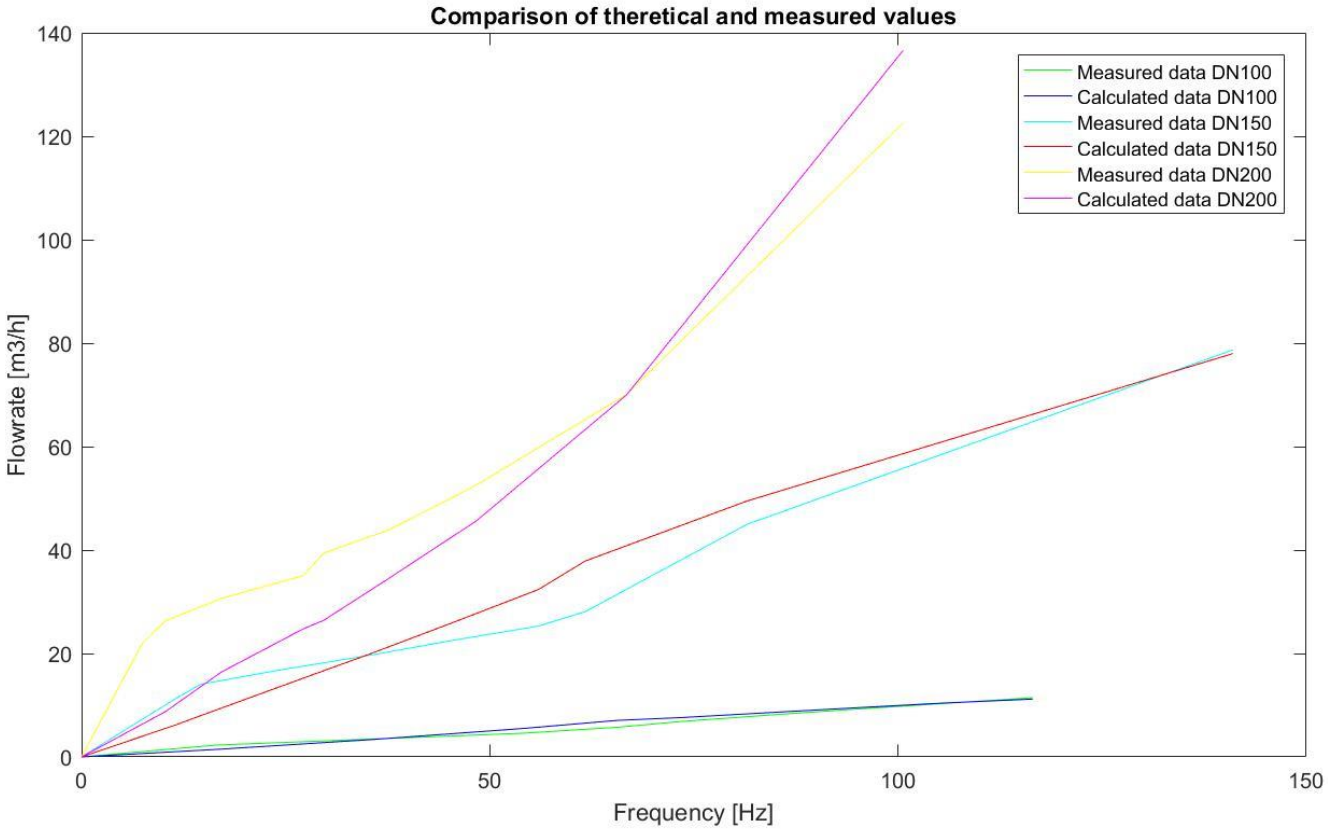

Figure 20: A comparison of calculated values of flow using the theoretical function.

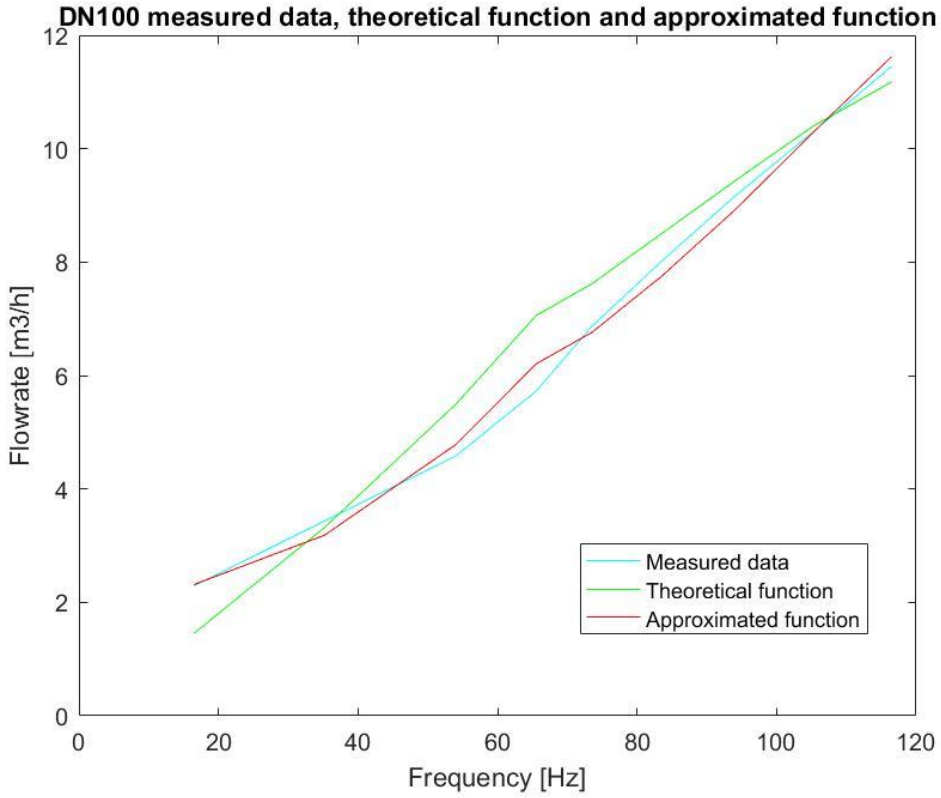

Figure 21: DN100 second degree polynomial approximation

Figure 21 above shows the closeness of flow functions for DN100 using alternative A (theoretical) and alternative B and C.

Table 2: Result DN100 Alternative A, B and C.

Approximated error DN100	**Maximum error [%]**	**Mean error [%]**
Theoretical function	36.5	11.8
2nd degree approximation	7.3	3.4
4th degree approximation	5.5	2.3
6th degree approximation	3.7	1.1
8th degree approximation	≈0	≈0

Table 2 shows the result of how accurate the methods can calculate the values compared to the measured values for DN100. Since both alternative B and C are based on approximations from measured data, the error of the flow rate functions of A and B in relation to measured flow is the same for all pipe sizes. It is only the degree of the approximated polynomial that determines the error.

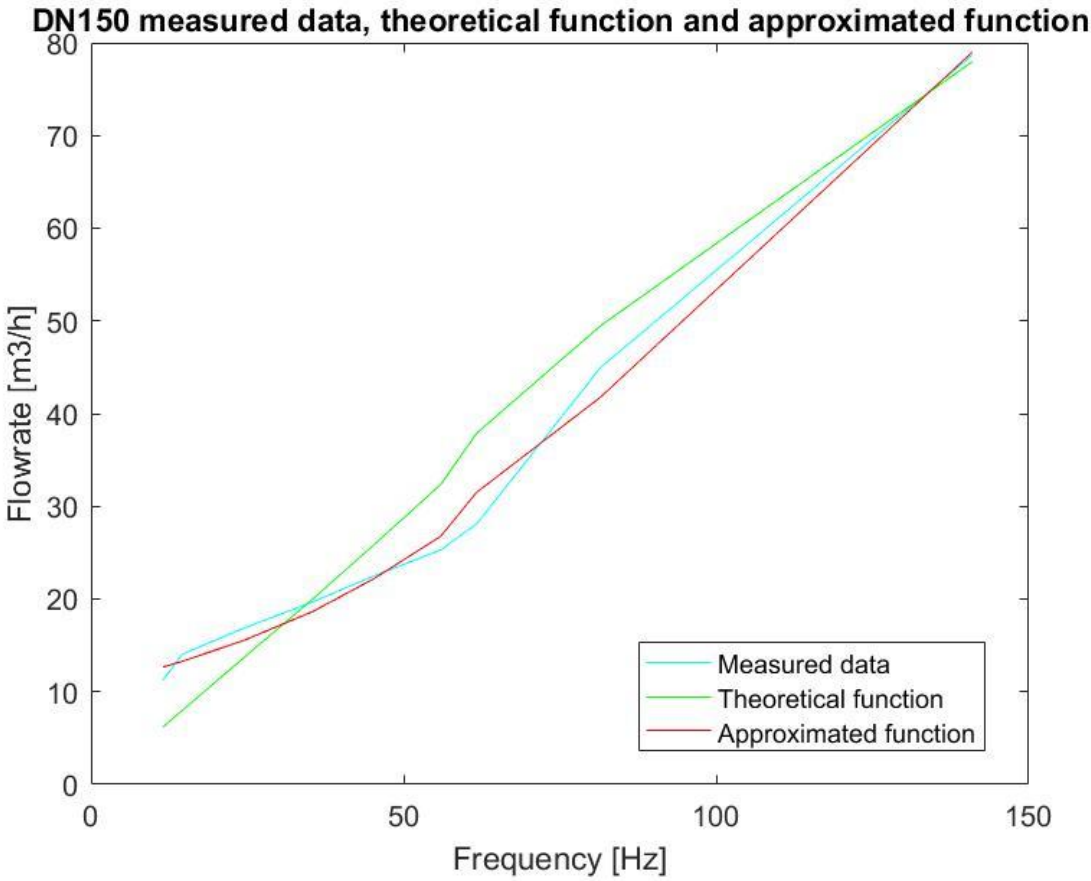

Figure 22: DN 150 second degree polynomial approximation.

Figure 22 above shows the closeness of flow functions for DN150 using alternative A (theoretical) and alternative B and C. The curves follow the same trends as DN100.

Table 3 Result DN150 Alternative A, B and C

Approximated error	**Maximum error [%]**	**Mean error [%]**
Theoretical function	45	21.9
2nd degree approximation	12.6	6.45
4th degree approximation	5	2.5
6th degree approximation	0.95	0.49
8th degree approximation	≈0	≈0

Table 3 shows the result on how accurate the methods can calculate the values compared to the measured values for DN150. The result follows the trends as for DN100 that the alternative B and C provides lower error than the purely theoretical flow.

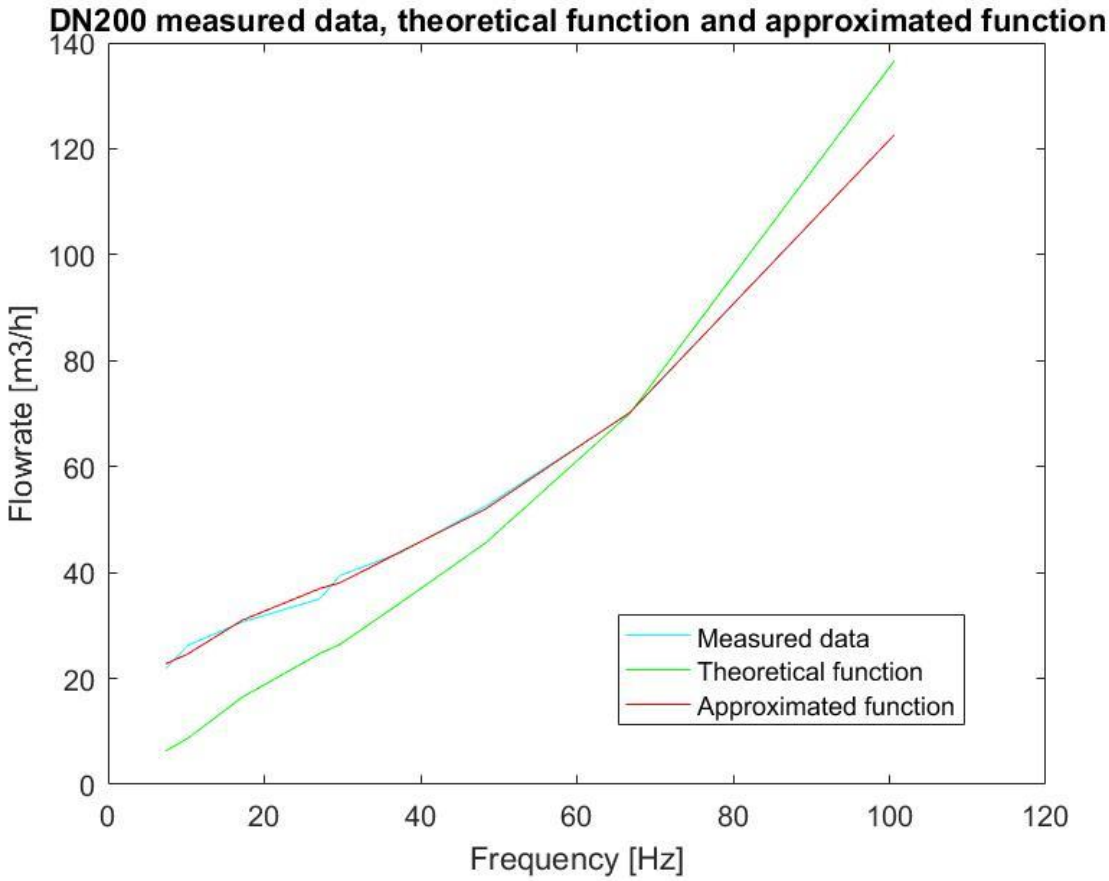

Figure 23: DN 200 second degree polynomial approximation

Figure 23 above shows the closeness of flow functions for DN150 using alternative A (theoretical) and alternative B and C. The curves follow the same trends as DN100.

Table 4 Result DN200 Alternative A, B and C

Approximated error DN200	**Maximum error [%]**	**Mean error [%]**
Theoretical function	71	29
2nd degree approximation	6	2.4
4th degree approximation	6	2.4
6th degree approximation	4.9	1.8
8th degree approximation	≈0	≈0

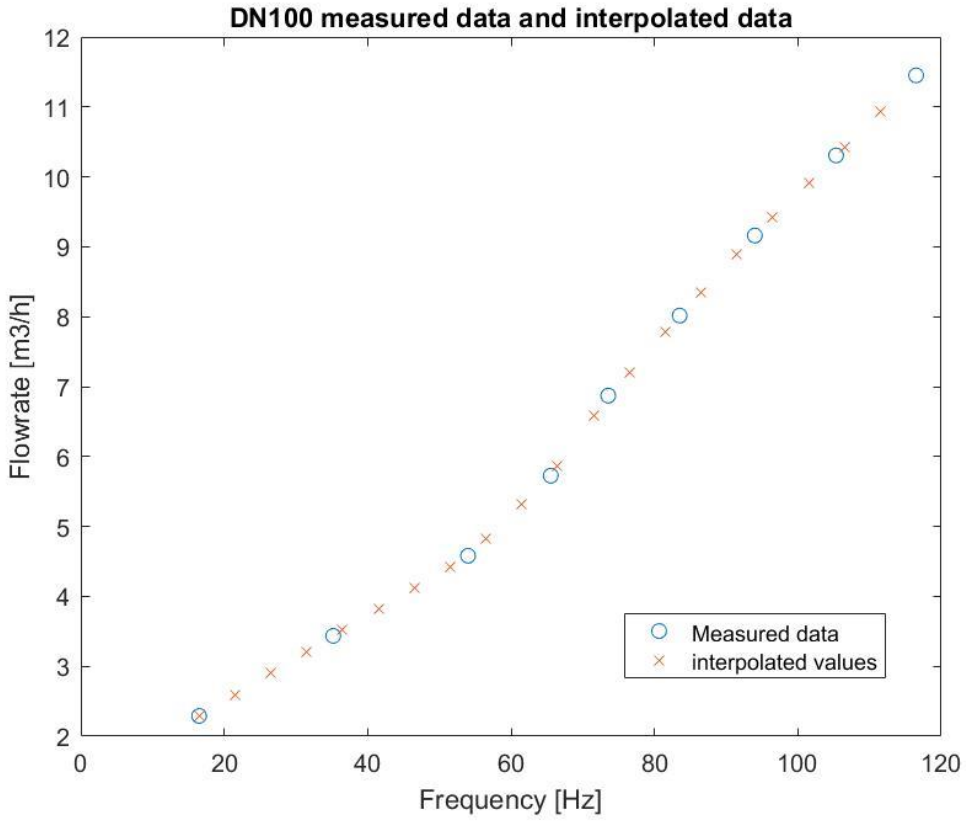

Figure 24: Interpolation DN100

Visual analyses were used to evaluate alternative D for all pipe sizes. Figure 24 shows the interpolated flow's compliance to the measured flow for DN100. Corresponding diagrams for DN200 and DN150 can be seen in Appendix 9.

7.2. Conducted hardware trials

Except for minor system checks and tests, two significant tests of the generator and the control circuit were conducted with the SimplexMotion motor rig.

7.2.1. Hardware trial 1

The results from the first hardware trial regarding load shedding are shown in table below.

Table 5 Load shedding verification

Load state	**Mean shaft torque**
Battery charging on, no external load	11.244 Nm
Battery charging off	10.064 Nm
Load reduction	10.5%
Battery charging on and 1A external load	21.956 Nm
Battery charging on and no external load	10.076 Nm
Load reduction	54.1%

7.2.2. Hardware trial 2

The result from the second hardware trial are shown in Table 6.

Table 6 Efficiency test

Pgen [W]	**Tshaft [Nm]**	**n [rpm]**	**ω [rad/s]**	**Pshaft [W]**	**efficiency**
0.019	0.02	93	9.7389	0.19477	0.09754
0.176	0.015	211	22.095	0.33143	0.53101
0.359	0.025	305	31.939	0.79848	0.44959
0.621	0.03	399	41.783	1.25349	0.49541
0.906	0.035	492	51.522	1.80327	0.50241
1.415	0.04	609	63.774	2.55097	0.55469
2.626	0.06	938	98.227	5.89362	0.44556
mean					0.49645

The mean efficiency was used for the derivation of the theoretical flow in Appendix 2.

8. Result analysis

This chapter evaluate the result and discusses the measured and calculated values. The collected data from trial 1 did not give enough values to give a precise function. Trial 2 contained more data and gave more precise functions and a possibility to draw some conclusions.

8.1. Trial 1

The visual compliance creates the impression that a second-degree polynomial fits the measured data well. But since there is an error of 13.7% for DN150 and 15.3% for DN200, it surpasses the maximum allowed error. A fourth-degree polynomial returns a lower error but it was still possible to improve further.

As seen Appendix Figure 1 in Appendix 1, the frequency was expected to be linear. But as seen in Figure 18 and Figure 19, the relationship does not seem to be linear.

8.2. Trial 2

A pattern was found (easily seen in Figure 20) that the measured flow is higher than the theoretical flow at lower flows and thereafter intersects the theoretical flow curve and was lower for higher flows. In DN150 and DN100 the last measured values were very close to the calculated values. The same curves are illustrated below, but for each DN-size in comparison to an approximative 2^{nd} degree function.

The purpose of Table 1 is to show the variations of *fgen* and *Pgen* for a flow on the test rig that varied with 10 l/h according to the rig's own flow meter. The variations were relevant to evaluate since they affect the variation of the returned theoretical flow when using alternative A for flow indication. The flow variation was negligible in relation to minimum measured flow of 1145 l/h on the test rig. The variation of 1-2 Hz is not always negligible in relation to a low flow with a generated frequency of e.g. 7 Hz. The variations in frequency with and without flow also indicated for DN100 and DN200 that rotation of the turbine was more stable with active battery charging. But it remains unclear if this stability was directly related to the electrical load caused by battery charging since it was only based on only one set of data. But one possibility was that an increased breaking torque increase the turbine wheels resistance to flow variation. The maximum achieved *Pgen* was not measurable for DN150 because of technical difficulties.

Seen in Figure 21, Figure 22 and Figure 23 is that even with the lowest degree of a polynomial, the curve follows the measured curve better than the theoretical curve.

The precision for the function of alternative D, i.e. linear interpolation, cannot be evaluated in the same way as the other alternatives were because there was no error in relation to the measured points. Therefore, the error of alternative D is fully dependent on the quality of the measured data.

Using a pure theoretical approach was abandoned after comparing it to the values collected in the trials and it did not reach the goal of maximum 15% error for any of the pipe dimensions.

The load shedding feature was tested during flow trial 2, where it didn’t show any significant difference in ability to measure low flows compared to during battery charge. The cause was later discovered to be fully charged batteries, which minimized the electrical load during *MODE_NORMAL*.

8.3. Hardware trials

The mean values of torque with and without battery charging and external electrical load indicated that the implemented load shedding feature worked (Table 5). The breaking torque was more than halved when the electric load was released, and that the breaking torque was reduced with about 11 % when the battery charging is deactivated.

9. Discussion

This chapter contains possible error sources, discussions about the alternatives for calculating the flow, thoughts about the code implementations and suggestions on how to continue to improve the work.

9.1. Possible error sources

It is difficult to predict the behavior of a physical process such as water flow through a pipe and signal transfer in electrical instruments. Some error sources are discussed below as for cause and suggestions of possible solutions.

9.1.1. Short circuit

The prototype that was tested during flow trial 1 did not have an insulating filling between the couplings of the stator coils to the phase wires. This caused leakage of fresh water within the cable insulation that emptied dropwise into the phase wire connector on the test rectifier. This may have affected the voltage between the phase-lines due to partial short-circuit between two phase wires, which in turn would have affected the voltage output from the rectifier. However, due to the sufficient amplitude of the phase signal, it is not likely that the decreased voltage would affect the ability to measure frequency between two phase lines. The problem was later solved in flow trial 2 by using silicon infill between the stator wires and the generator cord.

9.1.2. Electromagnetic interference

Using a Bench drill, servomotor and other devices that generates electromagnetic fields (EM-fields) near electrical instruments may be a source of inaccurate generator output due to induced current in the circuits. However, the devices used in this project have relatively low current and voltage ratings, making the interference negligible. This was verified by evaluating one of the phase signals with the oscilloscope. The primary prevention of EM interference is to avoid installing the product close to a powerful EM-source. In case this is not possible, electromagnetic shield cage is an option for the casing of the control circuit [27].

9.1.3. Meter fluctuations

The flow meter on the meter laboratory equipment shows a varying flow with a range of 10 l/h. Fluctuations in frequency are also detectable. These variations are probably caused by the equipment's flow meter precision, flow turbulence in the pipes and small mechanical, electromagnetic and electrical interferences on the control circuit. However, the flow variations are negligible in relation to the larger flows in which the generator was tested. In the same way, the range of variation for the frequency is negligible in relation to the tested generator rotational speeds. Turbulence can be avoided by placing the product in an optimal environment, sufficiently far away from curvature.

9.1.4. Hysteresis

In conducted flow trials, flow speed was changed from low to high. In trial two, it was noticed for mid-angle turbine that the flow rate needed to initiate spinning the turbine was higher than the flow where the turbine stops spinning. This indicates significant hysteresis, depending on increase or decrease and rate of flow change. Further investigation is required to eliminate errors caused by this effect. One possibility is to develop a feature in the software to predict the *flow* based on sign and amplitude of the flow rate's rate of change. However, this would require trials with data collection for a few controlled rates of change of both negative and positive sign.

To counter the "flow threshold" for rotation, one future possibility of development of the control circuit board is to add a motor driver circuit. It could be useful to transform the generator into a motor and "nudge" the turbine wheel with regular intervals when a certain period of time has passed since the rotor stopped because of a flow lower than the threshold flow.

9.1.5. Temperature fluctuations

In section 2.1 it was mentioned that seasonal fluctuations of the fresh water temperature may have an impact on the resulting rotational speed of the turbine. However, later acquired company data of computational fluid dynamics (CFD) simulations shows that only 1.5% of the Axial force consists of the visceral force, which makes a temperature fluctuation negligible.

9.1.6. Simplifications in theoretical model

The function for Q_{bias} in relation to *fgen* is partially based on the theoretical model derived in section 5.1, and it is based on certain simplifications and assumptions. These assumptions may contribute to the unpredictable error that defines the flow meter's bias error. CFD could be used to model the process using the parameters used in this project, but also with a wider range of less affecting parameters like temperature, pipe curvatures, etc.

9.1.7. Inaccurate product datasheets

When comparing the maximum error of the product to existing turbine flow meters, awareness must be made on how accuracy statements sometimes are twisted on the market to hide the flaws of a flow meter. The following statement is an example from a typical specification of a turbine flow meter [16]:

> **"Highly Accurate**
> NIST traceable factory calibration performed on every meter, within ±0.5%
> of reading accuracy at the calibrated (typical) flow velocity and within ±1-2%
> of reading over a 50:1 flow range.

Unequaled Operating Range
Provides repeatable flow data over a 175:1 turndown from 0.17 to 30 ft/s."

A reading error of ±0,5% may be true over a "typical" flow velocity used in the calibration procedure, but that velocity is still unspecified. The unstated calibration velocity might be several times higher than what the installation pipe is specified for, which creates a falsely wider work range and thus a smaller precision error. Furthermore, the flow rate over a 50:1 flow range means that the minimum velocity for a precision error of ±1-2% is 30[ft/s]/50 = 0,6 ft/s, which can be a common flow velocity and thus a substantial increase in precision error from ±0,5% to 1-2%. Also, the higher error of ±2% is more likely due to the increase in precision error at lower flows due to friction losses and such in the piping. That is why the first stated precision error of ±0,5% is not fully serviceable in this case [1].

9.2. Software differences

At first, Microsoft Office Excel was used both for datasheets and mathematical applications like approximating the polynomials used for alternative B and C. The polynomials were plotted in both MATLAB and excel and they had different characteristics. This was not further investigated, and MATLAB was used for all mathematical operations after flow trial 1.

To make the MATLAB scripts available for the company, the final versions was converted without bigger issues to be open in GNU Octave which is an open source software equivalent to MATLAB.

9.3. Programming

The already existing firmware of the product was developed by a consultant for the company and was used as a template for the programming. It required some time to get into the structure of the code. The memory is a problem where the maximum amount of words (10752) in the program is close to the limit which lead to problems when testing new functions in the code. This can be solved by using a better compilator that can compress the file more than the free version. Furthermore, optimisations can be made in the code.

9.4. Limitations in data collection

Due lack of time and technical problems, not all desired measurements were conducted to produce a desired result. In trial one, a technical error forced the trial to be stopped when measurements were made for DN150 and DN200. In trial two, the generated power was higher than expected, which activated the overvoltage protection. This affected the measurements and forced the test to be limited to lower flows than planned. Furthermore, in trial two, hysteresis was detected in low flows, which depended on previous rotational speed. This may also have affected some measurement data.

The conclusion from previously conducted flow trials was that generator frequency is a sufficient output value to calculate a good function. But after trial two, generated power was included in the measured data to include the electric load's impact on the calculated flow.

9.5. Previous company data collections

Data from a previously conducted flow trial (Appendix 1) were available to the authors, in which exponential relationships was shown between

- Flow rate and generated voltage, thus also power given a known resistive generator load (Appendix Figure 2).
- Turbine blade angle and generator frequency

And a linear relationship between generated frequency and flow rate seen in Appendix Figure 1, which according to [5] indicates a time invariant process without dynamic properties.

9.6. Optimization of measurement points

As seen in Appendix 11, the *amount* of measurement points was not the most important factor for creating a good approximation but rather *where* the measurement points were located. This was because the error offset was compared to the reference flow meter's value, so that a difference of 1 m^3/s was 10% at 10 m^3/s but only 1% at 100 m^3/s. To solve this, the closeness of measure points was higher between 0.1 and 0.5 m/s and thereafter lower. This way, a more precise function could be approximated at low flows without more measure points.

9.7. Evaluation of methods

9.7.1. Alternative A.

Why this method delivered such high error was believed to be because the used formulas did not take swirl into account. But the theoretical function was still useful for use in alternative C. The advantage with alternative A would was that no new measurements needed to be made when new turbines would be introduced.

9.7.2. Alternative B

This method was the function using an approximated polynomial to calculate the current flow. Due to the complexity of the process in the product's intended environment, this was a suitable approach for the problem. The advantage was that the method was simple to use to create a function, using trial data vectors of *flow* and *frequency*. The produced polynomial was very simple to implement in the microcontroller but required a software to create the polynomial. MATLAB was used in this project, and the company will hence use a program called Octave.

9.7.3. Alternative C

This method was a combination of alternative A and B, which produced the same result as alternative B. But the big advantage with this modification was that when a new turbine was produced with minor changes, the theoretical version changed with new geometric parameters and the error from the last version was reusable, making the new function with an acceptable error. This was not tested due lack of new versions of turbines and time for trials. This alternative had the same disadvantage as Alternative B and needed a software to create the polynomial.

Alternative B and C delivered the same results where the degree of the polynomial determined how accurate the approximation was. The lowest error was given with an eighth-degree polynomial for a set of trial data vectors with nine elements. It was therefore believed that a minimal error of an approximated polynomial was achieved with an approximated c grade polynomial for a trial data vector with $c+1$ number of measure points.

9.7.4. Alternative D

Using interpolation to calculate the *flow* between two measure points had a strong similarity to the measure points as seen in Figure 24. However, this result was irrelevant if the measure points were based only on a few datasets, and might hence not have been reliable. There were irregularities in the measurements that needed to be verified as pattern and not anomalies to verify this method. These irregularities were not considered when using an approximative polynomial, which unavoidably consists of continuous and smoothened curves of "raw" data with LS. Sharper curves will however affect the result when using interpolation.

If this method was implemented in the firmware, the MATLAB script seen in Figure 17 could've been implemented in the microcontroller but the vectors with measured values would be stored in arrays with values from the latest data collection. This would've been beneficial because only the vectors with measurements need to be replaced whenever an updated version of the turbine is created, tested and recorded. But the code takes up more program memory space and take more time to execute than using a premade function, even though execution time isn't an issue in this case. Also, this method has the same problem as Alternative C that it requires new measurement for updated turbines even after small changes.

9.8. Suggestion of improvement

To improve the result, more flow trial data is needed. This means data collection with smaller changes of flow to increase the number of measurement points and repeated trials for a single configuration to decrease impact of precision error. An increased knowledge about confidence intervals in statistic is recommended to future developers in this area to conduct an optimal number of measurements to achieve data vectors of higher quality and known reliability.

To verify the result, more trials need to be executed. More data need to be collected so that an estimation of how the frequency is fluctuating at different flows and confidence interval needs to be created for the measured data. All alternatives need to be verified in the right environment by comparing the *flow* measured by the generator and an external flow meter. The calculated error in 7.1.2 only shows the error in which the produced function measures the flow in the exact same situation as the trial data was collected. Therefore, it cannot be used to give a result of how well the generator works as a flow meter in repeated measurements. Due to technical difficulties with the test rig, the resulting functions was never verified in the test environment.

In the theoretical function, better values could be achieved through a more precise derivation of the area in which open flow occurs in DN150 and DN200. This is because the measurements from flow trial was later discovered to be collected with the turbine reaching down to the bottom of the pipe for a rotational stability in the z-axis, making the estimated green area in Appendix figure 3 an underestimation. However, since the column above the turbine inlet is cylindric, the flow deviation is gentler than what could be estimated by a two-dimensional shape, e.g. a rectangle.

The flow can go in both directions and the function created in this project can only calculate the flow in the "correct" direction, i.e. counterclockwise. The software has potential to detect what direction the rotor spins at, but measurements and a new function needs to be modelled with reverse flow.

Depending on the customer, the flow calculation feature in the software could be changed to measure the flow continuously instead of during a brief period, every 50 seconds. But this would require the load shedding to be deactivated during the measurements.

Load shedding could be evaluated more to see if it serves the purpose to give more exact values than if the load shedding is turned off in both low values of frequency and high values. Depending on battery status and thus the electrical load, load shedding could be activated for a variable limit of low flow rates. This would also be the limit where load shedding isn't needed for flows above the limit.

Flow trials for different blade angles could be conducted, with which an error polynomial (see alternative C) could be evaluated in how different pipe sizes and blade angles affect the

polynomial. This would decrease the need for new measurements depending on blade angle and pipe sizes and hopefully be less dependent on measured data.

The error of the function from alternative B and the interpolation table of alternative D can be decreased if a function of *Pgen* is integrated into the flow measure feature in addition to *fgen*. A suggestion on how to achieve this is using statistics, more precisely fractional factorial design to determine the effect, *I*, that flow rate have on generated power and generator frequency or a combination of both. Thereafter, an approximative function of flow could consist of several parts, one term for each factor [29]. See Equation 10 below:

$$Q = I_f Q(fgen) + I_P Q(Pgen) + I_{fP} Q(fgen, Pgen)$$

Equation 10: multifactorial approximative polynomial.

Lastly, a suggestion of improvement would be to implement a feature to set a configuration of turbine and pipe parameters, e.g. via Simplex Interface. This would simplify interfacing with the system without the need for direct firmware modifications. For this reason, three variables were added to the parameters.h file, FLOWAREA, FLOWANGLE and FLOWRATE, where only FLOWRATE have been used in the function so far. However, this could take up more program memory in the PIC than what is available.

10. Conclusion

More flow trial data is needed to conclude which method of signal conversion delivers the most accurate result. Using only a theoretical approach is not recommended by the authors because the substantial error value seen in the result. Alternative B (Approximated polynomial) and C (Theoretical function and approximated polynomial) provides a good result but requires more measurement to give a reliable flow indication. Alternative C is more recommended than alternative B because it might need less testing in the future than Alternative B. Alternative D (interpolation) delivers a visually good result but is dependent on reliable measure data, and verifications are needed before any conclusions can be made.

The result in error for the flow meter in this project is not comparable to flow meters on the market because of different methods of verification. However, the error is believed to be low enough to achieve the ability of overseeing the flow in a water supply network and to help detecting leakages.

Features of flow rate indication and load shedding have been implemented into the products firmware according to the objectives. Foundations and how-to's have been created for the company as well as suggestions for future work, e.g. increased user-friendliness via simplex interface for future customers.

Reference list

[1] Cadillac Meter. (2017-05-26). *The Truth About Flow Meter Accuracy Statements* [Online]. Available: http://cadillacmeter.com/the-truth-about-flow-meter-accuracy-statements/

[2] I. Boldea, "Chapter 6. Control of Synchronous Generators in Power Systems", in *Synchronous Generators, 2*nd ed. Taylor & Francis Group, LLC, 2016.

[3] I. Boldea, "Chapter 3. Prime Movers", in *Synchronous Generators, 2*nd ed. Taylor & Francis Group, LLC, 2016.

[4] K. Pandiaraj, P. Taylor, N. Jenkins & C. Robb, "Distributed Load Control of Autonomous Renewable Energy Systems" in *14 IEEE TRANSACTIONS ON ENERGY CONVERSION, VOL. 16, NO. 1*, MARCH 2001, pp. 14 -19.

[5] B. Thomas, "Givare och mätdon" in *Modern Reglerteknik, 4*th ed. Stockholm, Sweden: Liber AB, 2013, ch. 21.

[6] Microchip, "General Purpose, 16-Bit Flash Microcontrollers with XLP Technology Data Sheet" PIC24FV16KM204 Family, Maj 2012 [rev. Feb, Apr, Jul och Nov 2010 & Jan 2012].

[7] R. Grahn, P-Å. Jansson, "Kraftgeometri" in Mekanik – Statik och dynamik, 3rd ed. Printed by Elanders Poland, Poland 2013, ch. 1, p. 32.

[8] F. Wedel, J Thomas, S. Wilcox, G. Wischstadt, C. Forte, "Load Shed Control Module For Use With Electrical Generator", U.S patent 20130270908, Apr 17, 2012. Found in: https://patentimages.storage.googleapis.com/pdfs/06e0bcac668f439fa38b/US20130270908A1.pdf

[9] American Water Works Association (AWWA) "1. Characteristics of Flow" in *Flowmeters in Water Supply - Manual of Water Supply Practices, M33, 2*nd ed (2006), Denver. Online version available at: http://app.knovel.com/hotlink/pdf/id:kt0087WCJ2/flowmeters-in-water-supply/characteristics-flow

[10] American Water Works Association (AWWA) "2. Types of Flowmeters" in *Flowmeters in Water Supply - Manual of Water Supply Practices, M33, 2*nd ed (2006), Denver. Online version available at:

http://app.knovel.com/hotlink/pdf/id:kt0087WCS2/flowmeters-in-water-supply/types-of-flowmeters

[11] American Water Works Association (AWWA) “3. Flowmeter Selection” in *Flowmeters in Water Supply - Manual of Water Supply Practices, M33, 2*nd ed (2006), Denver. Online version available at: http://app.knovel.com/hotlink/pdf/id:kt0087WDX1/flowmeters-in-water-supply/flowmeter-selection

[12] Y. A. Çengel, J. M. Cimbala, R. H. Turner, ”Bernoulli and energy equations” in *Thermal-Fluid Sciences, 4*th ed. in SI units, McGraw-Hill Education / Asia, 2012, ch 12, pp 475 – 476.

[13] Y. A. Çengel, J. M. Cimbala, R. H. Turner, ”Properties of fluids” in *Thermal-Fluid Sciences, 4*th ed. in SI units, McGraw-Hill Education / Asia, 2012, ch 12, pp 431 – 433.

[14] Wikimedia Commons, Boundary layer separation (2017-05-05) [Online]. Available at: https://commons.wikimedia.org/wiki/File:Boundary_layer_separation.svg

[15] M. Holm, CTO of the company.

[16] ONICON. (2017-05-26). *Products - F-1200 Series - Turbine Flow Meters - Insertion* [Online]. Available: http://www.onicon.com/F1200.html

[17] Wikimedia Commons, Flujo-laminar-y-turbulento (2017-05-05) [Online]. Available at: https://commons.wikimedia.org/wiki/File:Flujo-laminar-y-turbulento.gif

[18] American Water Works Association (AWWA). “5. Communication, Information, and Signal Outputs” in *Flowmeters in Water Supply - Manual of Water Supply Practices, M33, 2*nd ed. (2006), Denver. Online version available at: http://app.knovel.com/hotlink/pdf/id:kt0087WDX1/flowmeters-in-water-supply/flowmeter-selection

[19] Alicat. (2017-01-25). *Technical Data for Alicat L - Series Liquid Flow Meters.* [Online]. Available: https://www.alicat.com/documents/specifications/Alicat_Liquid_Meter_Specs.pdf

[20] Endress + Hauser. (2017-05-05). *Technical Information Proline Promag 50H, 53H Electromagnetic flowmeter* [Online]. Available:

https://portal.endress.com/wa001/dla/5000319/0453/000/07/TI00048DEN_1416.pdf

[21] Siemens. (2017-05-26). *SITRANS F M MAGFLO 5000*, [Online]. Available: http://www.siemens.se/bu/as/pi/doc/broschyr_magflo.pdf

[22] Y. A. Çengel, J. M. Cimbala, R. H. Turner, ”Internal flow” in *Thermal-Fluid Sciences, fourth ed. in SI units*, McGraw-Hill Education / Asia, 2012, ch 14, p 540.

[23] Sverker Jacobson, ”Trefassystemet”, *Don för mekatronikprogrammet*, Gothenburg, Sweden, Section of signals and systems, 2016, ch. 4, pp 4 – 27.

[24] M. Mägi, K. Melkersson. ”Kraftverkan i remväxlar” in *Lärobok i Maskinelement,* 2017. EcoDev International AB, Gothenburg, Sweden.

[25] Wikimedia Commons, File:Rotating-3-phase-magnetic-field.svg. (2017-05-04) [Online]. Available at: https://commons.wikimedia.org/wiki/File:Rotating-3-phase-magnetic-field.svg

[26] MathWorks United Kingdom, Polynomial curve fitting - MATLAB polyfit,(2017-05-28), ,[Online], Available: https://se.mathworks.com/help/matlab/ref/polyfit.html

[27] S. Celozzi et al. Electromagnetic Shielding (1. Aufl.;1; ed.) 2008.

[28] Y. A. Çengel, J. M. Cimbala, R. H. Turner, ”Energy, energy transfer” in *Thermal-Fluid Sciences*, *4*th ed. in SI units, McGraw-Hill Education / Asia, 2012, ch. 3, p. 92.

[29] U. Dahlblom.”Reducerade försöksplaner” *Försöksplanering: faktorförsök.* 2003. Göteborg: Matematiklitteratur i Göteborg. ch. 3, p. 58.

Appendix 1 Data from previous trials

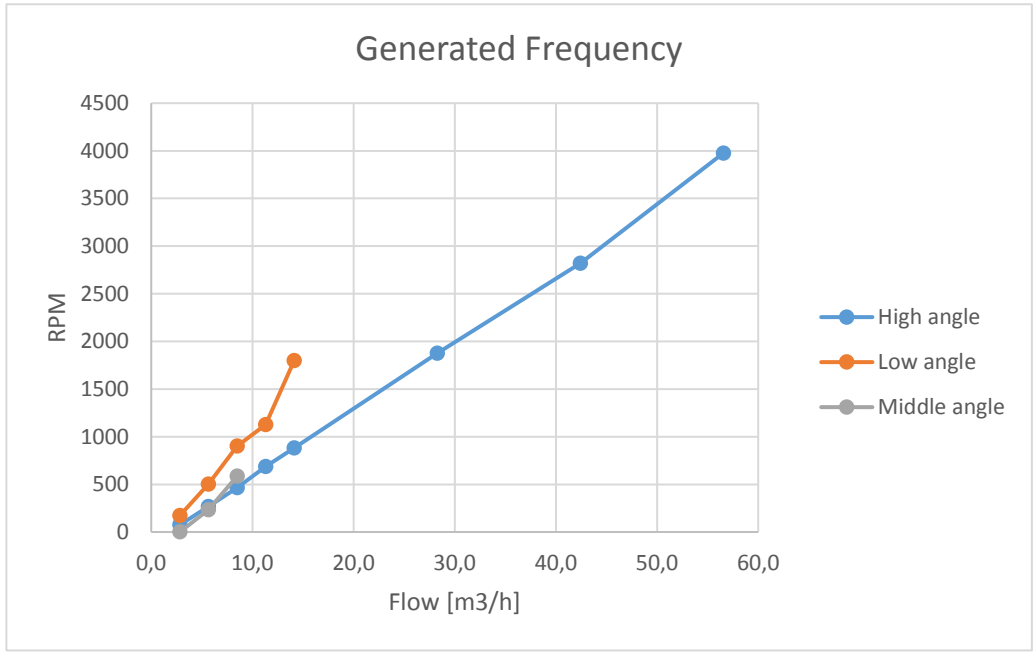

Appendix Figure 1 Graph for measured RPM and Flow

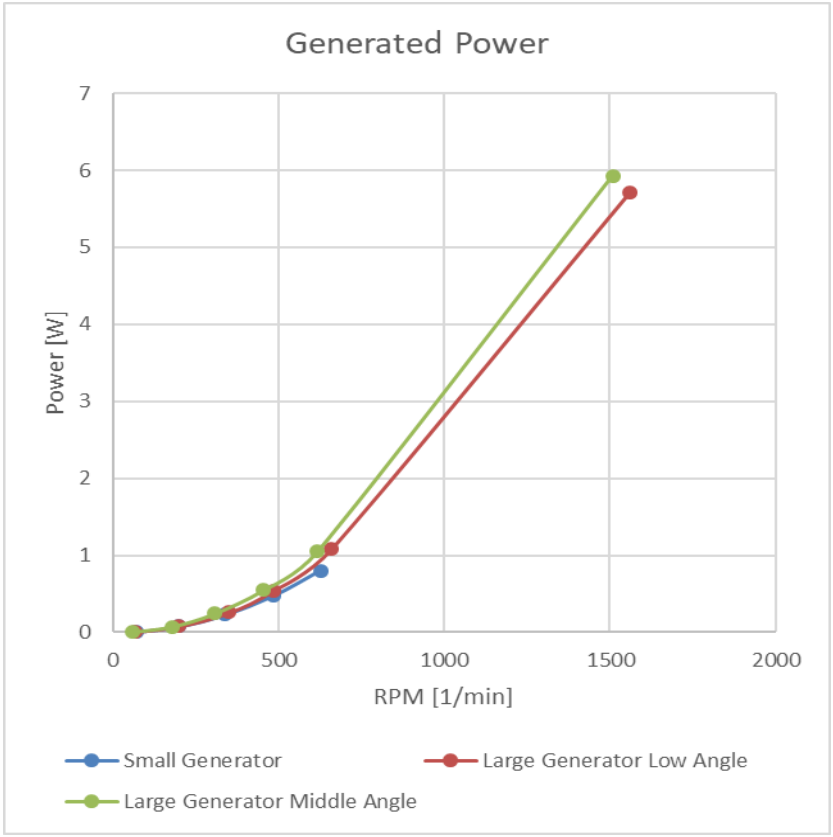

Appendix Figure 2 Graph for measured Power and RPM

Appendix 2 Theoretical function

Constants

Inner diameters of the used standard size pipes:

$D_{Pipe,DN100} = 90\ mm = \ 0{,}090\ m$
$D_{Pipe,DN150} = \ 140\ mm = 0{,}140\ m$
$D_{Pipe,DN200} = \ 175\ mm = 0{,}175\ m$

Stator width:

$D_{Stator} = 83{,}5\ mm\ = 0{,}0835\ m$

Inner boundary circle of the blade area (equivalent to hub diameter):

$D_{Blade,Inner} = \ 0{,}0300\ m$

Outer boundary circle of the blade area:

$D_{Blade,Outer} = \ 0{,}0588\ m$

Diameter of magnet array (measured from centre of mass):

$D_{Mag} = 65{,}5\ mm = 0{,}0655\ m$

Turbine inlet area is approximated as total blade area as follows:

$$A_{Blade} = \ \pi\left(\frac{D_{Blade,Outer}}{2}\right)^2 - \ \pi\left(\frac{D_{Blade,Inner}}{2}\right)^2 = \ 0{,}25\pi\left({D_{Blade,Outer}}^2 - \ {D_{Blade,Inner}}^2\right) \approx 0{,}00201\ m^2 = 20{,}1\ cm^2 \quad (1)$$

Average angle of blade used in this work:

$\alpha_{mid} = 26{,}5°$

Generator data:

Generator and full wave rectifier efficiency:

η_E = 0,4965 (see section 7.2.2 for measurement)

Number of rotor pole pairs: $N = 8$

Turbine data:

Torque caused by the water flow is collected from a parallel fluid simulation project of one turbine with an equivalent value of $D_{Blade,Outer}$. Assuming a mean total peripheral force on the blades of 1,4N [15], the resulting torque on the rotor is as follows [7]:

$$M_{Blades,Outer} = F_{Blade,Outer} \frac{D_{Blade,Outer}}{2} = 1{,}4 * 0{,}0295 = \ 0{,}041299 \text{ Nm}$$

Cross sectional open area parallel to turbine can then be approximated as a circle (marked with green in Appendix Figure 3) according to the following:

$$A_{Open} = \ A_{pipe} - \left(\frac{D_{Stator}}{2}\right)^2 \pi = A_{pipe} - 0{,}25\pi {D_{Stator}}^2 \quad (2)$$

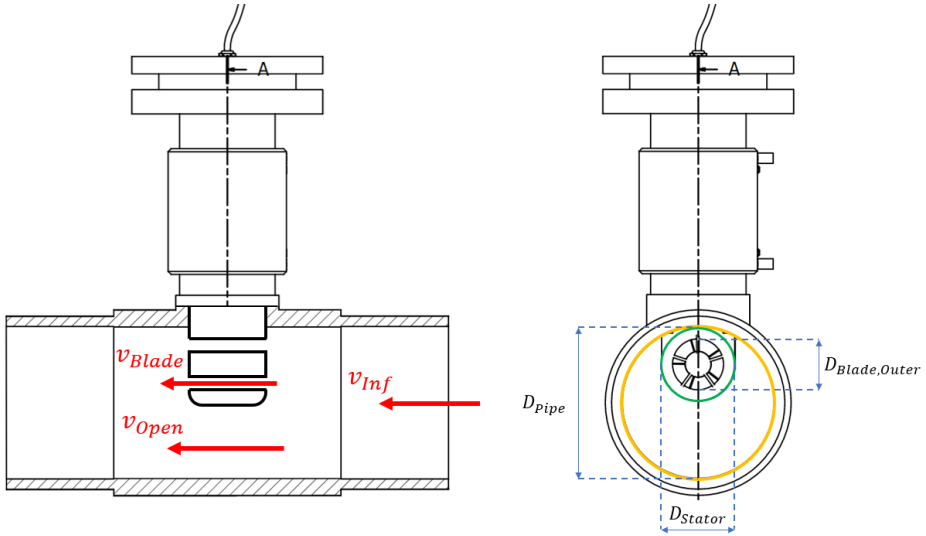

Appendix Figure 3 From left to right: Left side cross section view and front view of t-pipe with product installed.

Variables

Flow rate based on physical model and patched with bias error: $Q_{Total}\left[\frac{m^3}{h}\right]$

Flow rate based on physical model: $Q_{Theory}\left[\frac{m^3}{h}\right]$

Additional flow rate based on bias error (mapped through flow trial): $Q_{Bias}\left[\frac{m^3}{h}\right]$

Velocity of blade periphery: $v_{Blade,Outer}\left[\frac{m}{s}\right]$

Freestream velocity in pipe: $v_{Inf}\left[\frac{m}{s}\right]$

Freestream velocity through blade area: $v_{Blade}\left[\frac{m}{s}\right]$

Freestream velocity through open area: $v_{Open}\left[\frac{m}{s}\right]$

Generator frequency: $f[Hz]$

Generated power: $P_{Gen}\,[W]$

Derivation of Q_{Theory}:

The actual flow can be calculated as the theoretical flow complemented with the bias error as follows:

$$Q_{Total} = Q_{Theory} + Q_{Bias}$$

Where:

$$Q_{Theory} = 3600\left[\frac{s}{h}\right] A_{Pipe}\, v_{Inf}$$

Where, according to Bernoulli's principle, we have [12]:

$$A_{Pipe}v_{Inf} = A_{Blade}v_{Blade} + A_{Open}v_{Open} \rightarrow v_{Inf} = \frac{A_{Blade}V_{Blade} + A_{Open}V_{Open}}{A_{Pipe}} \quad (4)$$

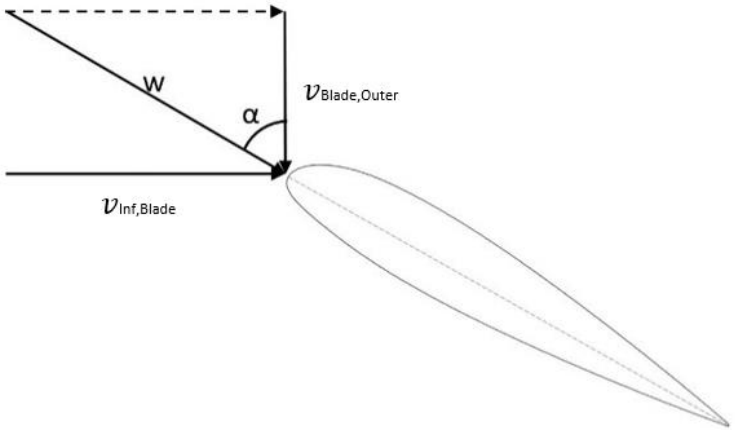

Appendix Figure 4 Velocity triangle. [15]

Where [15]:

$$v_{Blade} = v_{Blade,Outer} \tan(\alpha) \quad (5)$$

$$A_{Pipe} = \left(\frac{D_{Pipe}}{2}\right)^2 \pi = 0{,}25\pi {D_{Pipe}}^2 \quad (6)$$

Since the pressure drop is low, the axial flow speed is assumed the same through the turbine and through the bypass area, i.e.:

$$v_{Open} = v_{Blade} \quad (7)$$

Where the peripheral blade velocity depends on *fgen*, generated power and number of rotor polepairs according to the following derivation.

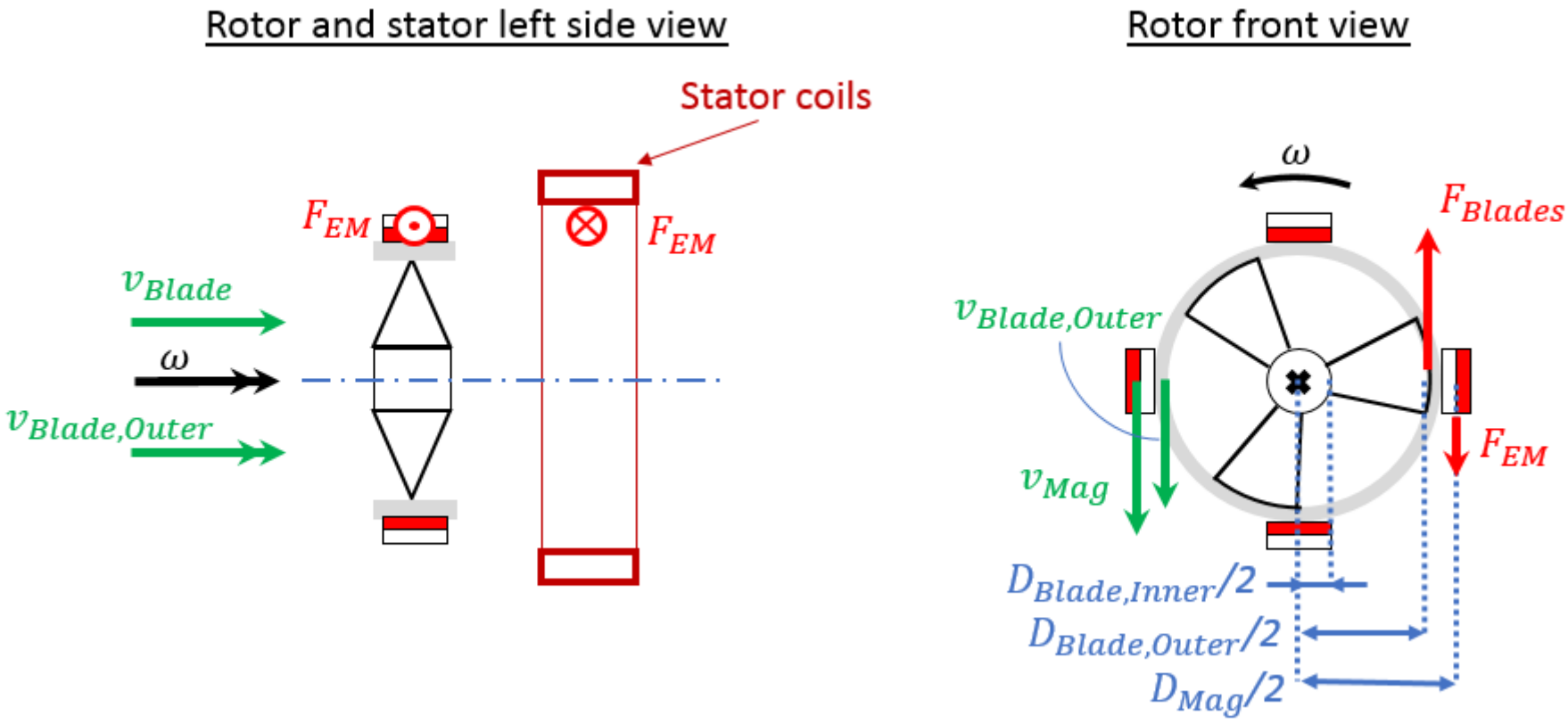

Appendix Figure 5 Free body diagram of generator rotor.

Torque balance gives (see Appendix Figure 5 above):

$$\sum \mathrm{M} = 0 \rightarrow M_{Blades,Outer} - M_{EM} = 0 \leftrightarrow F_{Blades,Outer} \frac{D_{Blade,Outer}}{2} - F_{EM} \frac{D_{Mag}}{2} = O$$

$$F_{EM} = F_{Blades,Outer} \frac{D_{Blade,Outer}}{D_{Mag}} \quad (8)$$

Where [24]

$$P_{EM} = F_{EM} v_{Mag} \quad (9)$$

$$P_{Mek} = F_{Blades,Outer} v_{Blade,Outer} \quad (10)$$

Where F_{Blades} and F_{EM} includes the sum of the peripheral forces on all the rotor's blades and magnets respectively.

The blades' peripheral speed $v_{Blade,Outer}$ is given through the following relationship [24]:

$$P_{Rotor,Tot} = P_{Mek} - P_{EM} = F_{Blades,Outer} v_{Blade,Outer} - F_{EM} v_{Mag}$$

$$P_{Rotor,Tot} = P_{Gen} \frac{1}{\eta_E} \rightarrow P_{Mek} - P_{EM} = P_{Gen} \frac{1}{\eta_E} \quad (11)$$

$$\omega = \frac{v_{Mag}}{D_{Mag}/2} = \frac{2\pi f}{N} \rightarrow v_{Mag} = \frac{\pi f D_{Mag}}{N} \quad (12)$$

MATLAB-script for derivation of function

```
syms APipe V P_Gen D_Pipe D_Stator D_BladeInner D_BladeOuter D_MagOuter MBladesOuter F_BladesOuter Q_th APipe VInf ABlade VBlade
VBladeOuter AOpen VOpen Alpha MBladesOuter MEm PEm FEm VMag PMek Omega f N PRotorTot PEm Eta VOpen QTheory

%Alpha = tand(v);



% PRotorTot = P_Gen / Eta;
%
% PRotorTot = PMek - PEm;
APipe = (D_Pipe/2).^2*pi; %(6)

AOpen = APipe - (D_Stator/2).^2 * pi; % (2)

VMag = pi * f * D_MagOuter / N; % (12)

FEm = F_BladesOuter * D_BladeOuter/D_MagOuter; %(8)

PEm = FEm * VMag; %(9)

PMek = P_Gen/Eta + PEm; % (11)

%PMek = FBladesOuter * VBladeOuter;

VBladeOuter = PMek / F_BladesOuter; % (10)

VBlade = VBladeOuter * Alpha; %(5) Alpha = tand(v)
```

```
VOpen = VBlade; %(7)

ABlade = 0.25 * pi * (D_BladeOuter.^2 - D_BladeInner.^2); %(1)

VInf = (ABlade*VBlade+AOpen*VOpen)/APipe; %(4)

QTheory = 3600*APipe*VInf; % (3)

simplify (QTheory)

pretty (simplify (QTheory))
```

The script returns the following:

ans =

-(900*Alpha*pi*(N*P_Gen + pi*D_BladeOuter*Eta*F_BladesOuter*f)*(D_BladeInner^2 - D_BladeOuter^2 - D_Pipe^2 + D_Stator^2))/(Eta*F_BladesOuter*N)

Which can be written as:

$$Q_{Theory} = 900\pi\tan(\alpha)\left(D_{Blade,Outer}{}^2 + D_{Pipe}{}^2 - D_{Stator}{}^2 - D_{Blade,Inner}{}^2\right)\left(\frac{P_{Gen}}{F_{Blades,Outer}\eta_E} + \frac{D_{Blade,Outer}\pi f}{N}\right)$$

Appendix 3 MATLAB script alternative B

```
%--------------------------------------------------------------------------
%   File Type:  Function to create an approximated polynomial
%   Created:    170327
%       Altered:
%   Author:     Karl Lindell
%   Contains:   Script for creating a mathematical model of flow rate
%               as a function of a variable frequency
%--------------------------------------------------------------------------

f = xlsread('C:\Resultatbok Labb 2.xlsx',1,'T10:T19')';    % Frekvens
Q = xlsread('C:\Resultatbok Labb 2.xlsx',1,'S10:S19')';   % Flöde
f=f./100; % För att frekvensen ska bli i Hz


P = polyfit (f,Q,4);                                          %Create a polynomial
Qc = polyval(P,f);                                           %Creates a vector with new values of flow



plot(f,Q,'r',f,Qc,'b');                                     %Plots the theoretical function and the
xlabel('Frequency [Hz]');
ylabel('Flow rate [m3/h]');
title('Function DN150')
legend('Measured data','Polynomial')


fprintf ('%0.5f * Gen_Freq*Gen_Freq * Gen_Freq*Gen_Freq + %0.5f * Gen_Freq*Gen_Freq*Gen_Freq %0.5f * Gen_Freq*Gen_Freq  + %0.5f * Gen_Freq
+ %0.5f \n', P(1),P(2),P(3),P(4),P(5))     %adjust to polynomial degree
```

Appendix 4 MATLAB script Alternative C

```
%--------------------------------------------------------------------------
%   File Name:
%   File Type:  Funktion för framställning av algorithm
%   Created:    170517
%       Altered:
%   Author:     Karl Lindell
%   Contains:   Script for creating a mathematical model of flow rate
%               as a function of a variable AC frequency and GenPower, for a given blade
%               angle and pipe diameter, in this case mid-angle and DN150
%
%   Input:
%   -  Datavector of flow rate: Q [m3/h]
%   -  Datavector of frequency: f [Hz]
%   -  Datavector of Power: P_Gen [Watt]
%   -  Mean blade angle: v [degrees] (constant)
%   -  Outer diameter of the blades: D_BladeOuter [m]
%   -  Inner diameter of the blades: D_BladeInner [m]
%   -  Pipe diameter: D_pipe [m] (constant)
%   -  Turbine stator width: D_stator [m] (constant) same as Dpipe in dn100 because no water is allowed to flow beside.
%   -  Diameter of magnet array (measured from center of mass): D_MagOuter [m]
%   -  the amount of polepairs in the generator: N
%   -  Generator and fullwave rectifier efficiency: Eta
%   Output:
%   -  calculated flow: Qth [m3/h]
%--------------------------------------------------------------------------

%Data gathering

f = xlsread('C:\Resultatbok Labb 2.xlsx',1,'X11:X19')';    % Frekvens
Q = xlsread('C:\Resultatbok Labb 2.xlsx',1,'W11:W19')';   % Flöde
P_Gen = xlsread('C:\ Resultatbok Labb 2.xlsx',1,'Y11:Y19')';
P_Gen = P_Gen./1000; % mW -> W
```

```
f=f./100; % 100 Hz -> 1 Hz

%Constants from pipes and turbine

v = 26.5;
D_Pipe = 0.175;
D_BladeOuter = 0.0588;
F_BladesOuter = 1.4;
D_BladeInner = 0.03;
D_Stator = 0.0835;
N = 8;
D_MagOuter = 0.0655;
Eta = 0.4965;
Alpha = 0.498;%tand(v);

%Calculations

Qth = -(900*Alpha*pi*(N*P_Gen + pi*D_BladeOuter*Eta*F_BladesOuter*f)*(D_BladeInner^2 - D_BladeOuter^2 - D_Pipe^2 +
D_Stator^2))/(Eta*F_BladesOuter*N);

E_offset = Q - Qth;                                                    %Error ( Reality - Theoretical value)
p = polyfit (f,E_offset,2);                                             %Create a polynomial
F = polyval(p,f);                                                       %Calculate the Error at each frequency
Qtot = Qth + F;

plot(f,Q,'c',f,Qth,'g',f,Qtot,'r');

xlabel('Frequency [Hz]');
ylabel('Flow rate [m3/h]');
title('DN200 measured data, theoretical function and approximated function');
legend('Measured data','Theoretical function','Approximated function');

start = 1; %where to start calculating the error
E = start:length(f); %Error vector
Em = 0;

for x=start:length(f)
  E(x) = (abs(Q(x) - Qtot(x))/Q(x))*100 % Creates a vector with the error
```

```
 Em = E(x)/length(f) + Em %Calculates the mean error
end


fprintf('Declare all variables from this program in MPLAB\n')
fprintf ('This is the Function for dn200: %0.5f * FrequencyActual*FrequencyActual + %.5f * FrequencyActual + %.5f -
(900*Alpha*3.14*(N*Param.GenPower + 3.14*D_BladeOuter*Eta*F_BladesOuter*FrequencyActual)*(D_BladeInner*D_BladeInner -
D_BladeOuter*D_BladeOuter - D_Pipe*D_Pipe + D_Stator*D_Stator))/(Eta*F_BladesOuter*N) \n', p(1),p(2),p(3));
```

Appendix 5 MATLAB - script Alternativ D

```
f = xlsread('C:\ Resultatbok Labb 2.xlsx',1,'R11:R19')';    % Frekvens
Q = xlsread('C:\ Resultatbok Labb 2.xlsx',1,'Q11:Q19')';   % Flöde
f=f./100; % 100 Hz -> 1 Hz

M = length(f); % Amount of measurements
Flow = f(1):5:f(M);
F = f(1):5:f(M); % Creates a vector to help us visualise the result
y = 1;
c = 1;

while y < length(F)+1 %First loop calculates the "measurement points"
    x = 2;
while x < M+1 %Second loop finds between what values to interpolate between
    if (F(y) < f(x)) % Checks if F(y) is less than f(x), when F(y) > f(x) it should interpolate.
        c = x;
        x = M;
    end
 x = x +1;
end
alpha = (F(y)-f(c-1))/(f(c)-f(c-1)); %Calculate the interpolation
Flow(y) = Q(c-1)+alpha * (Q(c)-Q(c-1)); %Calculate the interpolation
y = y + 1;
end

plot (f,Q,'o',F,Flow,'x') %Plot the result

xlabel('Frequency [Hz]');
ylabel('Flow rate [m3/h]');
```

```
title('DN100 measured data and interpolated data');
legend('Measured data','interpolated values');
```

Appendix 6 Flowcharts alternative B and C

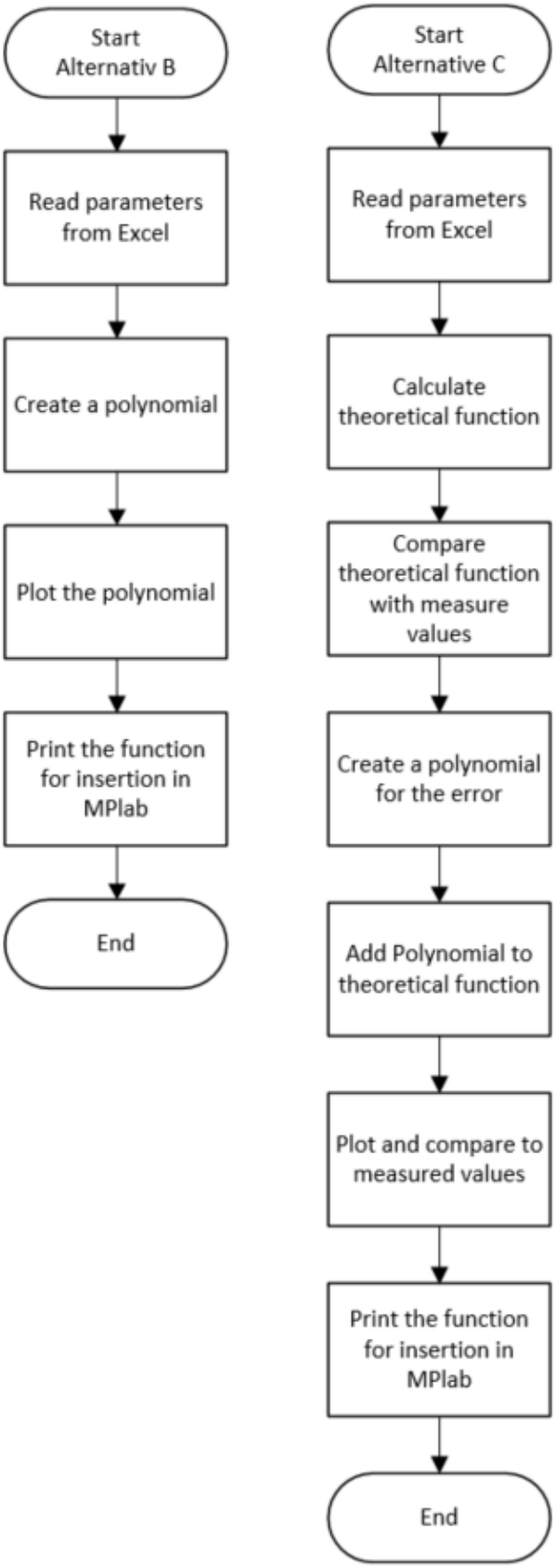

Appendix 7 Flowchart for analysis of alternative D

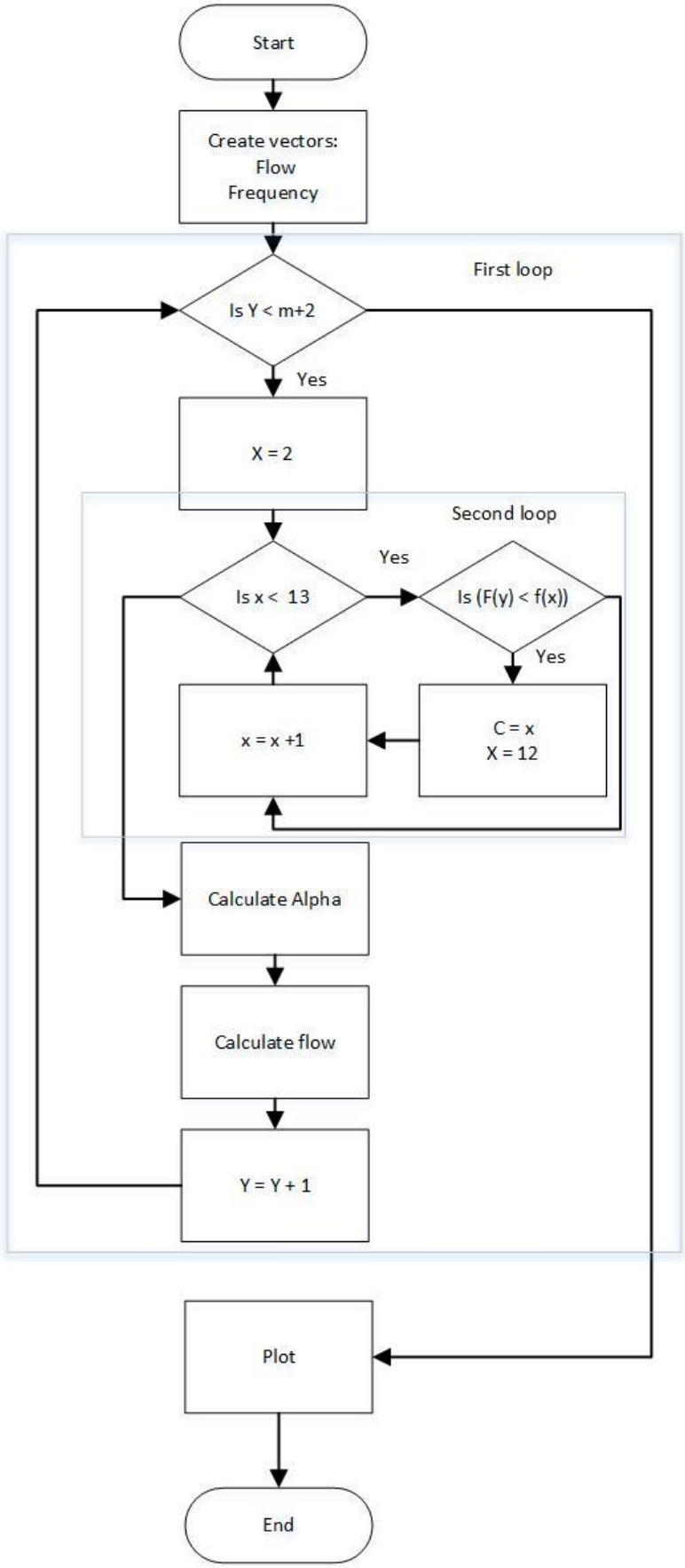

Appendix 8 Flowchart for flow measurement

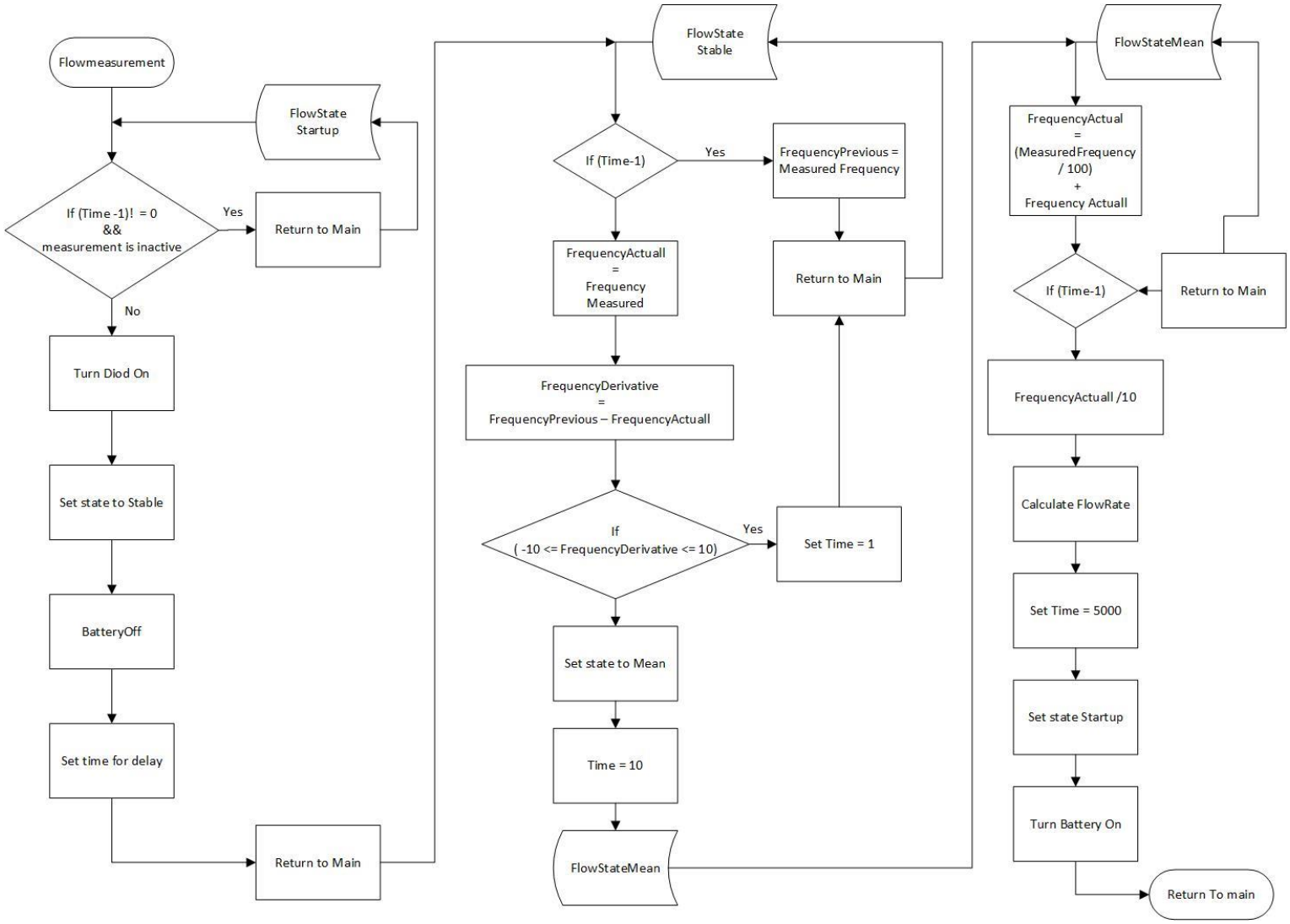

Appendix 9 Interpolation DN150 and DN200

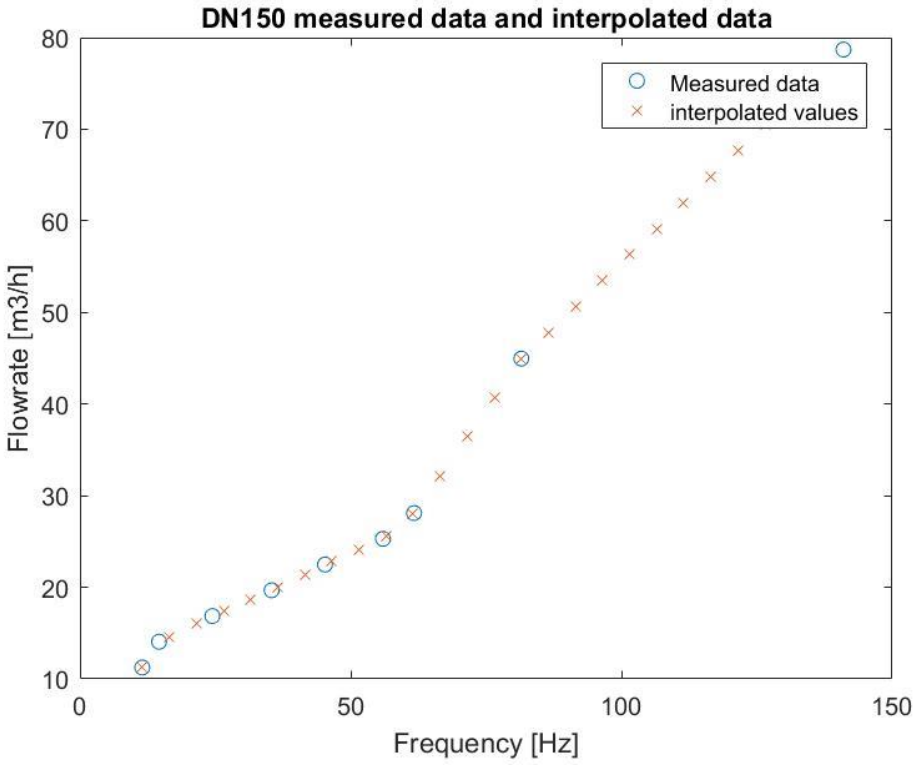

Appendix Figure 6 Interpolation DN150

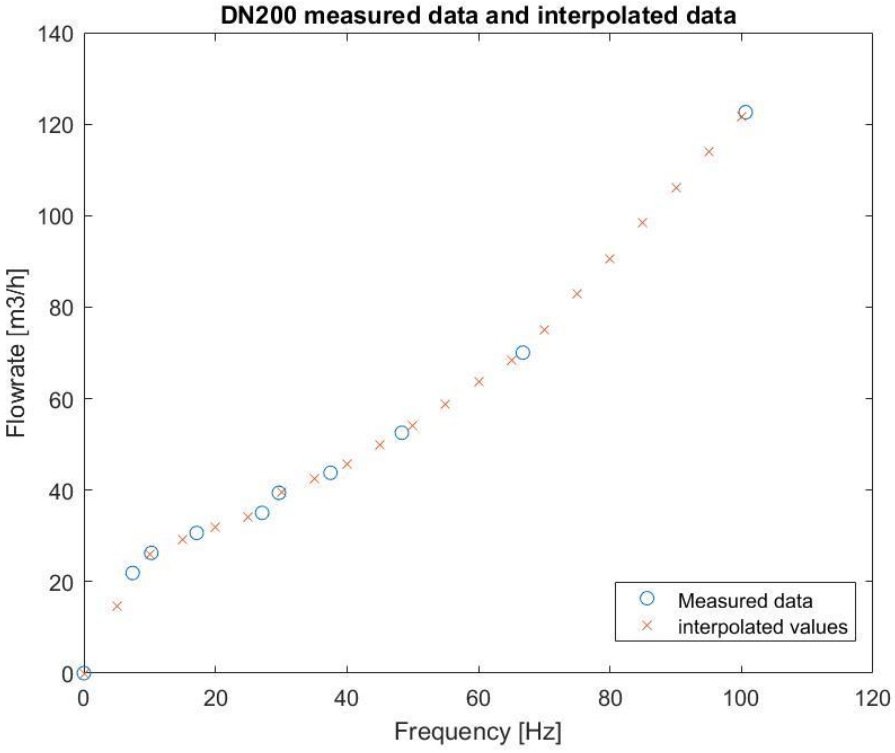

Appendix Figure 7 Interpolation DN200

Appendix 10 Verification of polynomial

Creating the polynomial

Using Excel's feature polynomial trendline, the data from the measurements was used to create four 2nd degree polynomials that describes the relations flow rate $Q \rightleftharpoons$ generator voltage U and flow rate $Q \rightleftharpoons$ turbine rotational speed n (simply referred to as speed in this appendix) for DN150 and DN200 (see Appendix table 1 and Appendix table 2).

	Dn150	Dn200
$\boldsymbol{n \rightarrow Q}$	$Q = -0{,}00003n^2 + 0.0902n + 5.3657$	$Q = -0{,}00009n^2 + 0{,}2142n + 14{,}754$
$\boldsymbol{U \rightarrow Q}$	$Q = -0{,}0166U^2 + 2{,}3191U + 8{,}0078$	$Q = -0{,}0866U^2 + 6{,}5497U + 15{,}989$
$\boldsymbol{Q \rightarrow U}$	$U = 0{,}0069Q^2 + 0{,}0903Q - 0{,}0099$	$U = 0{,}0019Q^2 - 0{,}0118Q + 0{,}3088$
$\boldsymbol{Q \rightarrow n}$	$n = 0{,}0941Q^2 + 9{,}128Q - 67{,}506$	$n = 0{,}0289Q^2 + 2{,}6984Q - 38{,}293$

Appendix table 1: functions for DN100 and DN200.

Verification and tweaking

The polynomials reliability from flow trial 1 needed to be verified, which is why an "unofficial" hardware test was conducted to determine the voltage for a given speed. The same speed on the rotor was set and the output voltage was measured. Then the polynomials in Appendix table 1 were used for calculating the corresponding flow Q given a value of n. Then the polynomials were used to calculate the corresponding voltage U to the current flow. This procedure was used for both DN 150 and DN 200. The opposite procedure, converting from voltage to flow and flow to RPM was also tested for both pipe diameters.

Verification of polynomials

Appendix table 2 shows the error in polynomials when transferring from $n \rightarrow Q \rightarrow U$ and $U \rightarrow Q \rightarrow n$.

	DN160		DN200	
n	n → U error [%]	U → n error [%]	n → U error [%]	U → n error [%]
200	33,0	1,99	37,1	9,20
300	24,8	4,04	21,2	12,8
400	16,5	4,93	9,66	13,8
500	9,65	5,61	1,77	13,4
600	5,02	5,86	2,54	11,6
700	1,82	5,35	4,64	8,14
800	0,280	4,29	4,97	3,09

Appendix table 2: Error in calculated values

This result was not used in the project but it gave a hint whether the method with second-degree polynomial approximations was an appropriate method to use for reconstructing flow rate values.

Appendix 11 Optimization of measurements

Every time a new turbine is produced a new function is needed. To reduce the time it takes to test a new turbine, the amount of tests was optimized to as few measurement points as possible without losing to much precision. Six different plots were compared with one “actual” curve consisting of 20 measurement points. Every plot had a different distribution and amount of measurement points between 0,1 and 2,0 m/s. The plots were used to create polynomials from the measurements that was compared to the optimal polynomial. See Appendix Figure 8 for comparison of 8 and 20 measured points and how it affects the result of the approximated polynomial.

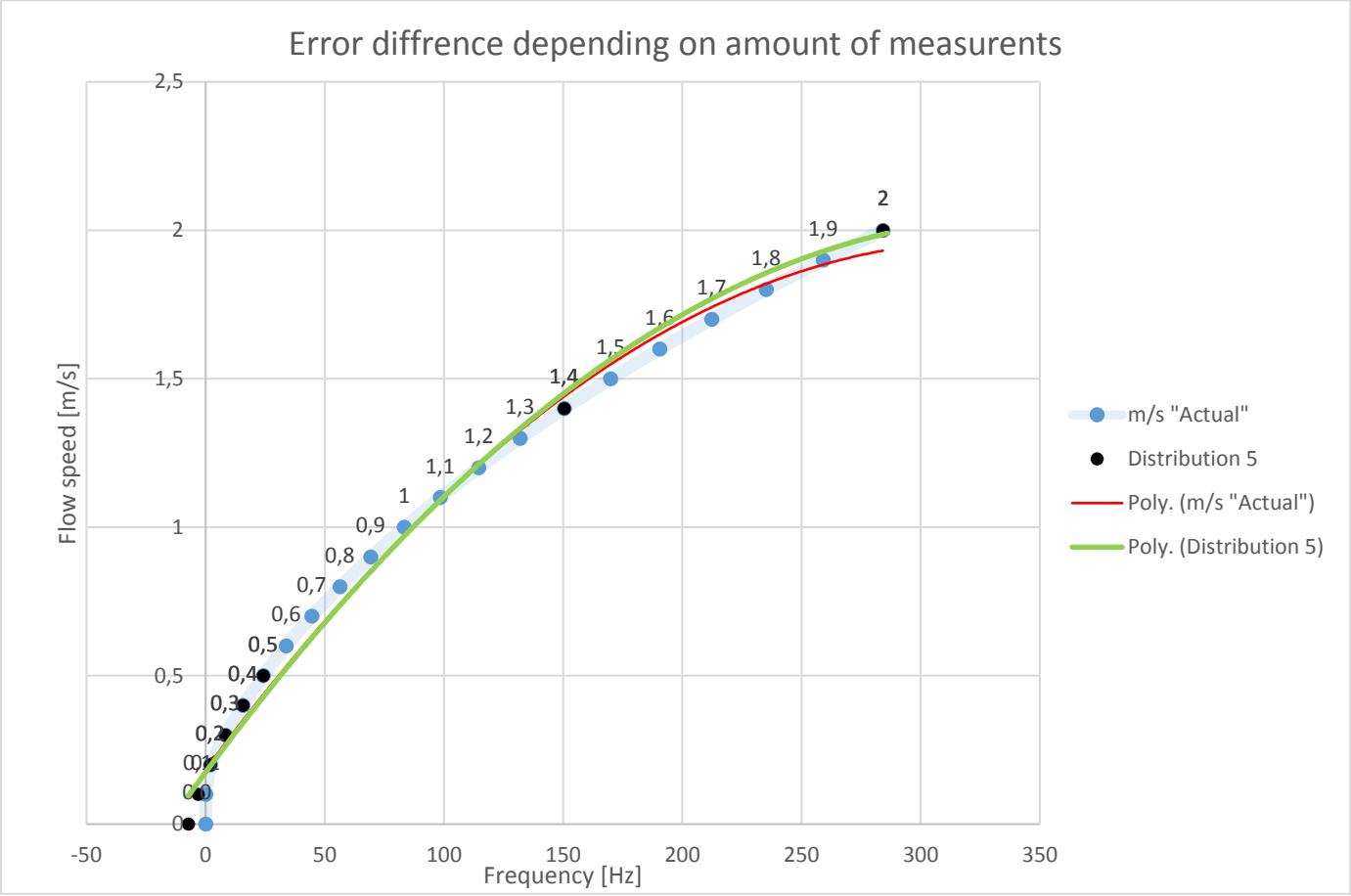

Appendix Figure 8 Optimization of measurement points

The blue dots together with the black are the 20 measurement points and the black are the 8 ones used in distribution 5. The red curve is a polynomial approximated from the blue and black dots while the green curve is approximated from the black dots.

MATLAB was used to validate how precise the polynomials was and what the biggest differ was from the optimal function. See Appendix 12 for the script used in MATLAB.
The result is that the maximal error is 4.6 % and this happens at 1 Hz but when the graph gets closer to 10 Hz where the actual turbine starts spinning its down to 2.5 %.

Appendix 12 MATLAB script optimization of measurement points

```
f=@(x)-(2*10.^(-5)) * x.^2 + 0.0109*x + 0.1746; %Polynom som ska jämföras Konfig 5
just nu
g=@(x) -(2*10.^(-5)) *x.^2 + 0.0108*x + 0.1837; % Facit

x = linspace (0,284); % Plottar mellan 0 och 284. 284 är frekvensen som motsvarar 2,0
m/s
plot (x,g(x),'b',x,f(x),'r');% Plottar polynomen brevid varandra

x = 1; % Besämmer startpunkten för mätningarna
z = 0; %felet i procent
y = 0; %vid vilket x-värde största felet uppstår
m = 0; %medelfelet
c =0;
kmax = 284 - x; %antalet itterationer förslagsvis lika många som frekvensen

for k=0:kmax

    d = abs(f(x)-g(x)); % Totala felet
    c = d / g(x); % Felet i procent jämfört med värdet
    m = m + c; % adderar felet till ett medelfel

   if z < abs(f(x)-g(x))/(g(x)) % Om felet är större än föregående fel
       p = abs(f(x)-g(x)); % Totala felet
       z = p / g(x); % Felet i procent jämfört med värdet
       y = x; %sparar x värdet vid största felet
   end

   x = x+1;
end
m = m/kmax;
disp ([z,y,p,m])%Skrive ut Felet i procent, vid vilket xvärde felet uppstod och hur
stort det var.
```